

Enclosure 5

**Vogtle Electric Generating Plant
Request for Technical Specifications Amendment
Steam Generator Tube Surveillance Program**

**Westinghouse Electric Company LTR-CDME-06-58-NP
“Steam Generator Tube Alternate Repair Criteria for the
Portion of the Tube Within the Tubesheet at the Vogtle 1 & 2
Electric Generating Plant for One Cycle Application”
dated July 11, 2006 - Non-Proprietary Version**

**Steam Generator Tube Alternate Repair Criteria
for the Portion of the Tube Within the Tubesheet
at the Vogtle 1 & 2 Electric Generating Plant
for One Cycle Application**

July 11, 2006

Author: /s/ Gary W. Whiteman

Gary. W. Whiteman

Regulatory Compliance and Plant Licensing

Signing for Gary W. Whiteman

* N. R. Brown

N. R. Brown

Steam Generator Design and Analysis

Verified: /s/ *Robert F. Keating

Robert F. Keating

Major Component Replacements & Engineering

Westinghouse Electric Company LLC

P.O. Box 355

Pittsburgh, PA 15230-0355

© 2006 Westinghouse Electric Company LLC

All Rights Reserved

This page intentionally blank.

Abstract

Nondestructive examination indications of primary water stress corrosion cracking were found in the Westinghouse Model D5 Alloy 600 thermally treated steam generator tubes at the Catawba 2 nuclear power plant in the fall of 2004. Most of the indications were located in the tube-to-tubesheet welds with a few of the indications being reported as extending into the parent tube. In addition, a small number of tubes were reported with indications about 3/4 inch above the bottom of the tube within a region referred to as the tack-expansion, and multiple indications were reported in one tube at internal bulge locations in the upper third of the tubesheet. The tube end weld indications were dominantly axial in orientation and almost all of the indications were concentrated in one steam generator. Circumferential cracks were also reported at internal bulge locations in two of the Alloy 600 thermally treated steam generator tubes at the Vogtle 1 plant site in the spring of 2005. Internal tube bulges within the tubesheet are created in a number of locations as an artifact of the manufacturing process. Based on interpretations of requirements published by the NRC staff in GL 2004-01 and IN 2005-9, the Southern Nuclear Operating Company (SNC) requested that a recommendation be developed for examination of the tubesheet regions of the steam generator tubes at the Vogtle 1 & 2 Electric Generating Plant for 1R13 and 1R12, respectively. An evaluation was performed that considered the requirements of the ASME Code, Regulatory Guides, NRC Generic Letters, NRC Information Notices, the Code of Federal Regulations, NEI 97-06, and additional industry requirements. The conclusions of the technical evaluation are that:

- 1) the structural integrity of the primary-to-secondary pressure boundary is unaffected by tube degradation of any magnitude below a tube location-specific depth ranging from 2.3 to 7.0 inches depending on the tube leg and bundle zone being considered, designated as H*, and,
- 2) that the accident condition leak rate integrity can be bounded by twice the normal operation leak rate from unlimited degradation below 17 inches from the top of the 21 inch thick tubesheet, including degradation of the tube end welds.

These results follow from analyses demonstrating that the tube-to-tubesheet hydraulic joints make it extremely unlikely that any operating or faulted condition loads are transmitted below the H* elevation, and the contact pressure dependent leak rate resistance increases below the neutral plane within the tubesheet. The possibility of degradation at such locations in the Vogtle 1 & 2 steam generator tubes exists based on the reported degradation at Catawba 2 and previously at Vogtle 1. The determination of the required engagement depth was based on results from finite element model structural analyses and a steam line break to normal operation comparative leak rate evaluation. It was also concluded that the evaluation of the conditions on the hot leg would always bound those for the cold leg with regard to leak rate performance. The cold leg requirements are greater than the hot leg requirements with regard to pullout resistance (the above numbers bound both). Application of the structural analysis and leak rate evaluation results to eliminate inspection and/or repair of tube indications in the region of the tube below 17 inches from the top of the tubesheet is interpreted to constitute a redefinition of the primary-to-secondary pressure boundary relative to the original design of the SG and requires the approval of the NRC staff through a license amendment.

This page intentionally blank.

Table of Contents

1.0	Introduction.....	9
2.0	Summary Discussion	14
3.0	Historical Background Regarding Tube Indications in the Tubesheet.....	17
4.0	Design Requirements for the Tube-to-Tubesheet Joint Region.....	19
5.0	Structural Analysis of Tube-to-Tubesheet Joint	21
6.0	Leak Rate Analysis of Cracked Tube-to-Tubesheet Joints.....	23
7.0	Conclusions.....	32
8.0	References.....	34
A.1	Evaluation of Tubesheet Deflection Effects for Tube-to-Tubesheet Contact Pressure	36
	A.1.1 Material Properties and Tubesheet Equivalent Properties.....	36
	A.1.2 Finite Element Model	38
	A.1.3 Tubesheet Rotation Effects.....	39
	A.1.4 Vogtle 1 & 2 Contact Pressures.....	43
A.2	Tube-to-Tubesheet Hydraulic Expansion Joint Crevice Depth	45
A.3	Determination of Required Engagement Length of the Tube in the Tubesheet	45
A.4	References.....	49

List of Tables

Table A-1.	Summary of Material Properties Alloy 600 Tube Material	51
Table A-2.	Summary of Material Properties for SA-508 Class 2a Tubesheet Material.....	51
Table A-3.	Summary of Material Properties SA-533 Grade A Class 2 Shell Material.....	51
Table A-4.	Summary of Material Properties SA-216 Grade WCC Channelhead Material.....	52
Table A-5.	Tube/Tubesheet Maximum & Minimum Contact Pressures and H* Depths for Vogtle 1 & 2 Steam Generators	53
Table A-6.	Cumulative Forces Resisting Pull Out from the TTS Vogtle 1 & 2 Hot Leg Normal Conditions – 0% SGTP, $P_{sec} = 810$ psig	54
Table A-7.	Cumulative Forces Resisting Pull Out from the TTS Vogtle 1 & 2 Hot Leg Normal Conditions – 10% SGTP, $P_{sec} = 935$ psig	55
Table A-8.	Cumulative Forces Resisting Pull Out from the TTS Vogtle 1 & 2 Faulted (SLB) Conditions, $P_{sec} = 0$ psig	56
Table A-9.	Cumulative Forces Resisting Pull Out from the TTS Vogtle 1 & 2 FLB Conditions, 0% SGTP	57
Table A-10.	Cumulative Forces Resisting Pull Out from the TTS Vogtle 1 & 2 FLB Conditions, 10% SGTP	58
Table A-11.	Summary of H* Calculations for Vogtle 1 & 2	59
Table A-12.	H* Summary Table Structural Criteria Required Engagement.....	60
Table A-13.	Model F Pullout Test Data	61
Table A-14.	Model F 0.25 Inch Displacement Data at 600°F.....	61

List of Figures

Figure 1-1. Distribution of Indications in SG A at Catawba 2	12
Figure 1-2. Distribution of Indications in SG B at Catawba 2.....	12
Figure 1-3. Distribution of Indications in SG D at Catawba 2	13
Figure 2-1. As-Fabricated & As-Analyzed Tube-to-Tubesheet Welds	16
Figure 6-1. Loss Coefficient Values for Model F Leak Rate Analysis.....	28
Figure 6-2. Change in Contact Pressure at 20.0 Inches Below the TTS.....	29
Figure 6-3. Change in Contact Pressure at 16.9 Inches Below the TTS.....	29
Figure 6-4. Change in Contact Pressure at 12.6 Inches Below the TTS.....	30
Figure 6-5. Change in Contact Pressure at 10.5 Inches Below the TTS.....	30
Figure 6-6. Change in Contact Pressure at 8.25 Inches Below the TTS.....	31
Figure 6-7. Change in Contact Pressure at 6.0 Inches Below the TTS.....	31
Figure A-1. Definition of H* Zones (Vogtle Units 1 and 2).	62
Figure A-2. Finite Element Model of Model F Tubesheet Region.....	63
Figure A-3. Contact Pressures for NOp at Vogtle 1 & 2, 0% SGTP, $P_{sec} = 810$ psig	64
Figure A-4. Contact Pressures for NOp at Vogtle 1 & 2, 10% SGTP, $P_{sec} = 935$ psig	64
Figure A-5. Contact Pressures for SLB Faulted Condition at Vogtle 1 & 2	65
Figure A-6. Contact Pressures for FLB Condition at Vogtle 1 & 2, 0% SGTP	65
Figure A-7. Contact Pressures for FLB Condition at Vogtle 1 & 2, 10% SGTP	66

This page intentionally blank.

**Steam Generator Tube Alternate Repair Criteria
for the Portion of the Tube Within the Tubesheet
at the Vogtle 1 & 2 Electric Generating Plant for One Cycle Application**

1.0 Introduction

Indications of cracking were reported from the nondestructive, eddy current examination of the steam generator (SG) tubes during the fall 2004 outage at the Catawba 2 nuclear power plant operated by the Duke Power Company, References 1, 2, and 3. The tube indications at Catawba 2 were reported about 7.6 inches from the top of the tubesheet in one tube, and just above the tube-to-tubesheet welds in a region of the tube known as the tack expansion (TE) in several other tubes. Moreover, indications were also reported in the tube-end welds (TEWs), also known as tube-to-tubesheet welds, joining the tube to the tubesheet, with a small number of those indications extending into the tube material. The spatial distribution of indications by row and column number is shown on Figure 1-1 for SG A, Figure 1-2 for SG B, and Figure 1-3 for SG D at Catawba 2; there were no indications in SG C. The Catawba 2 plant has Westinghouse designed, Model D5 SGs fabricated with Alloy 600TT (thermally treated) tubes. Subsequently, indications were reported at the Vogtle Unit 1 plant operated by the Southern Nuclear Operating Company (Reference 4). The Vogtle 1 & 2 SGs are of the Westinghouse Model F design with slightly smaller diameter and thickness A600TT tubes than in the Catawba 2 Model D5 SGs. It was concluded from those observations that there is the potential for similar tube indications to be reported during future inspections of the Vogtle 1 & 2 SGs.

Note: No indications of this type were found during the planned inspections of the Braidwood 2 SG tubes in April 2005, a somewhat similar inspection of the tubes in two Model F SGs at Wolf Creek in April 2005, or an inspection of the Model D5 tubes at Comanche Peak 2 in the spring of 2005. Furthermore, no indications of this type were found during similar inspections of the Model D5 tubes at Byron 2 and Model F tubes at Vogtle 2 in the fall of 2005.

The SGs at the Model D5 plant sites were fabricated in the 1978 to 1980 timeframe using similar manufacturing processes with a few exceptions. For example, the fabrication technique used for the installation of the SG tubes at Braidwood 2 would be expected to lead to a much lower likelihood for crack-like indications to be present in the region known as the tack expansion relative to Catawba 2 because a different process for effecting the tack expansions was adopted prior to the time of the fabrication of the Braidwood 2 SGs.

The Model F SGs were fabricated in the 1979 through 1988 timeframe using similar manufacturing processes also with a few exceptions. The manufacturing procedures and drawing requirements indicate that the urethane expansion process was used during the manufacture of the Vogtle Unit 1 and 2 steam generators. Therefore, tack expansion transition inspection results similar to Catawba Unit 2 are judged unlikely to occur.

The findings in the Catawba 2 and Vogtle 1 SG tubes present three distinct issues with regard to future inspections of A600TT SG tubes which have been hydraulically expanded into the tubesheet:

-
- 1) indications in internal bulges within the tubesheet (created in a number of tubes as an artifact of the manufacturing process),
 - 2) indications at the elevation of the tack expansion transition, and,
 - 3) indications in the tube-to-tubesheet welds, including some extending into the tube.

The scope of this document is to:

- a) address the applicable requirements, including the original design basis, Reference 5, and regulatory issues, Reference 6, and,
- b) provide analysis support for technical arguments to limit tube inspection in the tubesheet region to an area above which degradation could result in potentially not meeting the SG performance criteria, i.e., the depths specified in Appendix A of this report. The analysis discussed herein demonstrates that the 17 inch inspection depth of the steam generator tubes from the top of the tubesheet using a rotating probe coil planned for implementation at Vogtle Units 1 and 2 is conservative.

An evaluation was performed that considered the requirements of the ASME Code, Regulatory Guides, NRC Generic Letters, NRC Information Notices, the Code of Federal Regulations, NEI 97-06, and additional industry requirements. The conclusion of the technical evaluation is that:

- 1) the structural integrity of the primary-to-secondary pressure boundary is unaffected by tube degradation of any magnitude below a tube location-specific depth designated as H^* , and,
- 2) the accident condition leak rate integrity can be bounded by twice the normal operation leak rate from degradation below 17 inches from the top of the 21 inch thick tubesheet.

These results follow from analyses demonstrating that the tube-to-tubesheet hydraulic joints make it extremely unlikely that any operating or faulted condition loads are transmitted below the H^* elevation, and that the tube-to-tubesheet contact leak rate resistance increases below the 17 inch elevation from the top of the tubesheet. The determination of the required engagement depth was based on the use of finite element model structural analyses and of a bounding leak rate evaluation based on the change in contact pressure between the tube and the tubesheet between normal operation and postulated accident conditions. The results provide the technical rationale to eliminate inspection of the region of the tube below 17 inches from the top of the tubesheet. Such an approach is interpreted to constitute a redefinition of the primary-to-secondary pressure boundary relative to the original design of the SG and requires the approval of the NRC staff through a license amendment.

A similar type of Technical Specification change was approved, on a one-time basis, to limit inspections of the Wolf Creek Model F and Braidwood 2 Model D5 SGs during the spring 2005 inspection campaigns, for example see References 7 and 8 respectively. Subsequent approvals were also obtained for use at Byron 2 and Vogtle 2 for their fall 2005 inspection campaigns, Reference 9 for example for the latter. This report was prepared to justify the specialized probe, e.g., RPC (rotating probe coil), exclusion zone to the portion of the tube below 17 inches from the top of the tubesheet based on meeting the structural and leak rate performance criteria for both the

hot and cold leg, and to provide the necessary information for a detailed NRC staff review of the technical basis for that request.

The H^* values were determined to assure meeting the structural performance criteria for the operating SG tubes as delineated in NEI 97-06, Revision 2, Reference 10. Compliance is based on demonstrating both structural and leakage integrity during normal operation and postulated accident conditions. The structural model was based on standard analysis techniques and finite element models as used for the original design of the SGs and documented in numerous submittals for the application of criteria to deal with tube indications within the tubesheet of other models of Westinghouse designed SGs with tube-to-tubesheet joints fabricated by other techniques, e.g., explosive expansion.

All full depth expanded tube-to-tubesheet joints in Westinghouse-designed SGs have a residual radial preload between the tube and the tubesheet. Early vintage SGs involved hard rolling which resulted in the largest magnitude of the residual interface pressure. Hard rolling was replaced by explosive expansion which resulted in a reduced magnitude of the residual interface pressure. Finally, hydraulic expansion replaced explosive expansion for the installation of SG tubes, resulting in a further reduction in the residual interface pressure. In general, it was found that the leak rate through the joints in hard rolled tubes is insignificant. Subsequent testing demonstrated that the leak rate resistance of explosively expanded tubes was not as great as that of hard rolled tubes and prediction methods based on empirical data to support theoretical models were developed to deal with the potential for leakage. The same approach was followed to develop a prediction methodology for hydraulically expanded tubes. However, the model has been under review since its inception, with the intent of verifying its accuracy because it involved analytically combining the results from independent tests of leak rate through cracks with the leak rate through the tube-to-tubesheet crevice. The leak rate model associated with the initial development of H^* to meet structural performance criteria is such a model; technical acceptance could be time consuming since it has not been previously reviewed by the NRC staff. An alternative approach, provided in this report, was developed for application at Vogtle 1 & 2 from engineering expectations of the relative leak rate between normal operation and postulated accident conditions based on a first principles engineering evaluation.

A summary of the evaluation is provided in Section 2.0 of this report. The historical background and design requirements for the tube-to-tubesheet joint are discussed in Sections 3.0 and 4.0 respectively. Section 5.0 addresses the structural analysis of the tube-to-tubesheet joint. Section 6.0 discusses the leak rate analysis, and finally, the conclusions from the structural and leak rate evaluations are contained in Section 7.0.

SG - 2A +Point Indications Within the Tubesheet

Catawba EOC13 DDP D5

E 1 INDICATION WITHIN 0.25" OF HOT LEG TUBE END
 ■ 66 PLUGGED TUBE

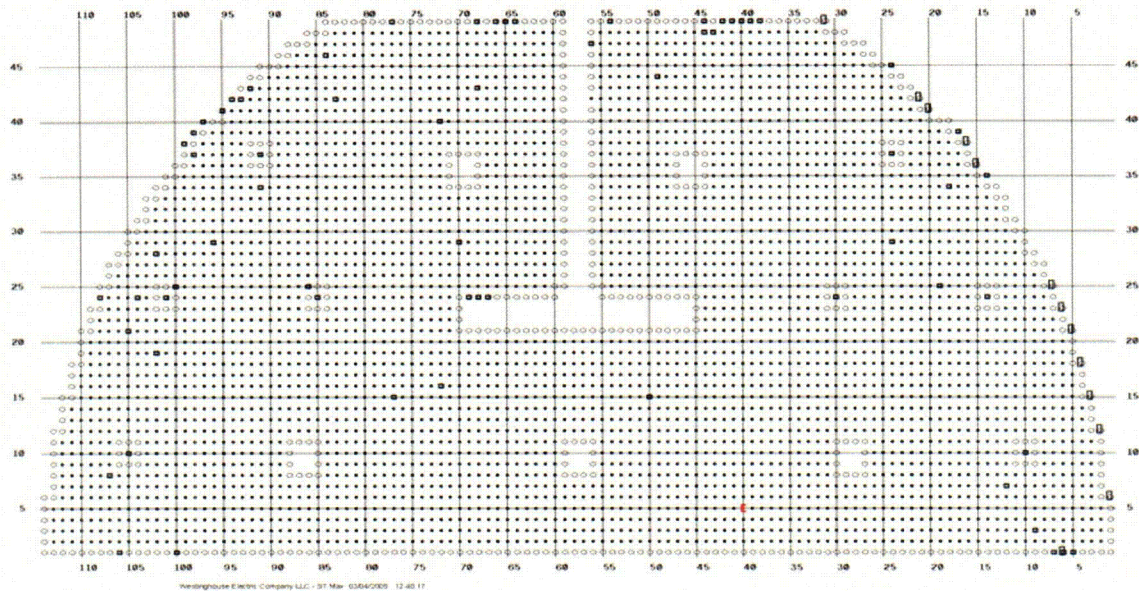


Figure 1-1. Distribution of Indications in SG A at Catawba 2

SG - 2B +Point Indications Within the Tubesheet

Catawba EOC13 DDP D5

Z 1 MULTIPLE INDICATIONS AT APPROXIMATELY 7" BELOW HOT LEG TOP OF TUBESHEET
 W 1 INDICATIONS WITHIN 0.25" AND BETWEEN 0.26" AND 0.80" OF HOT LEG TUBE END
 B 9 INDICATION BETWEEN 0.26" AND 0.80" OF HOT LEG TUBE END
 E 192 INDICATION WITH 0.25" OF HOT LEG TUBE END
 ■ 58 PLUGGED TUBE

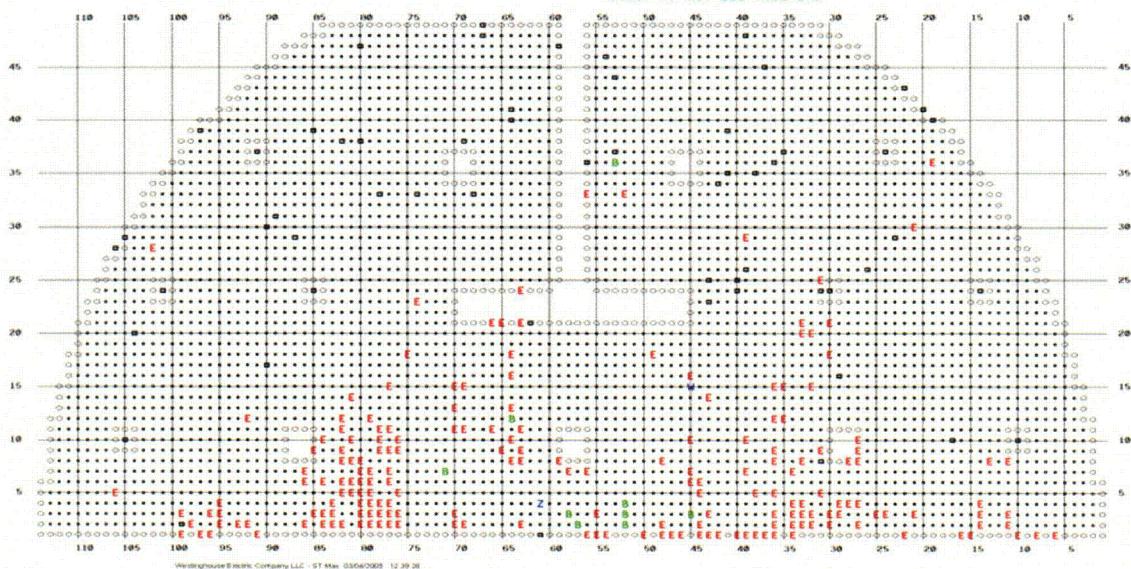


Figure 1-2. Distribution of Indications in SG B at Catawba 2

C.OI

SG - 2D +Point Indications Within the Tubesheet

Catawba EOC13 DDP D5

E 7 INDICATION WITHIN 0.25" OF
HOT LEG TUBE END
■ 85 PLUGGED TUBE

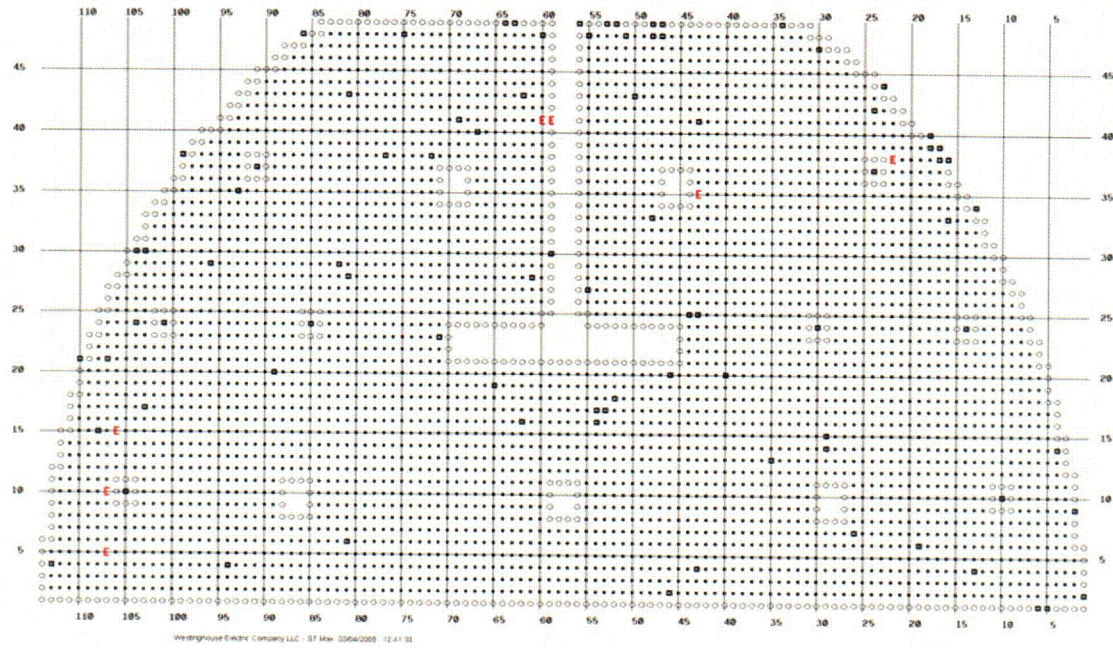


Figure 1-3. Distribution of Indications in SG D at Catawba 2

C-02

2.0 Summary Discussion

Evaluations were performed to assess the need for addressing degradation in the region of the SG tubes within the tubesheet at the Vogtle 1 & 2 Electric Generating Plant. The conclusions from the evaluation are that a redefinition of the pressure boundary can be effected while still assuring that the structural and leak rate performance criteria would be met during both normal operation and limiting postulated accident conditions.

Implementation of the redefinition of the pressure boundary results in the elimination of the examination of the tubes below a depth on the order of 17¹ inches from the top of the tubesheet, which includes eliminating the need to inspect the region of the SG tubes referred to as the bottom of the expansion transition (BET), the region of the tube-to-tubesheet joint referred to as the tack expansion, and the tack expansion transition near the bottom of the tubesheet. In addition, consideration was given to the need to perform inspections of the tube-to-tubesheet weld in spite of the fact that the weld is specifically not part of the tube in the sense of the plant technical specification, see Reference 2. It is concluded that there is no need to inspect the tube-to-tubesheet welds for degradation because the tube in these regions has been shown to meet structural and leak rate criteria regardless of the level of degradation. The results from the evaluations performed as described herein demonstrate that the inspection of the tube within about 10 inches of the tube-to-tubesheet weld and of the weld is not necessary for structural adequacy of the SG during normal operation or during postulated faulted conditions, nor for the complying with leak rate limits during postulated faulted events.

In summary:

- The structural integrity requirements of NEI 97-06, Reference 10, are met by sound tube engagement lengths ranging from 2.3 to 7.0 inches from the top of the tubesheet, thus the region of the tube below those elevations, including the tube-to-tubesheet weld is not needed for structural integrity during normal operation or accident conditions.
- NEI 97-06, Reference 10, defines the tube as extending from the tube-to-tubesheet weld at the tube inlet to the tube-to-tubesheet weld at the tube outlet, but specifically excludes the tube-to-tubesheet weld from the definition of the tube. The acceptance of the definition by the NRC staff was recorded in the Federal Register on March 2, 2005, Reference 11.
- The welds were originally designed and analyzed as primary pressure boundary in accordance with the requirements of Section III of the 1971 edition of the ASME Code, Summer 1972 Addenda, References 5, 12 and 13. The analyses are documented in Reference 12 for the Vogtle 1 & 2 SGs. The typical as-fabricated and the as-analyzed weld configurations are illustrated on Figure 2-1.

¹ The depth value specified corresponds to the worst location in the tubesheet and is considerably less towards the periphery.

- Section XI of the ASME Code, Reference 14 (1971) through 15 (2004), deals with the inservice inspection of nuclear power plant components. The ASME Code specifically recognizes that the SG tubes are under the purview of the NRC through the implementation of the requirements of the Technical Specifications as part of the plant operating license.

The hydraulically expanded tube-to-tubesheet joints in Model F SGs are not leak-tight without the tube end weld and considerations were also made with regard to the potential for primary-to-secondary leakage during postulated faulted conditions. However, the leak rate during postulated accident conditions would be expected to be less than that during normal operation for indications near the bottom of the tubesheet (including indications in the tube end welds) based on the observation that while the driving pressure increases by about a factor of almost two, the flow resistance increases because the tube-to-tubesheet contact pressure also increases. Depending on the depth within the tubesheet, the relative increase in resistance could easily be larger than that of the pressure potential. Therefore, the leak rate under normal operating conditions could exceed its allowed value before the accident condition leak rate would be expected to exceed its allowed value. This approach is termed an application of the "bellwether principle." While such a decrease in the leak rate is rationally expected, the postulated accident leak rate could conservatively be taken to be bounded by twice the normal operating leak rate if the increase in contact pressure is ignored. Since normal operating leakage is administratively limited (by NEI 97-06) to be less than 0.1 gpm (150 gpd) in the Vogtle Units 1 and 2 SGs, the attendant accident condition leak rate, assuming all leakage to be from the lower tubesheet indications, would be bounded by 0.2 gpm in the faulted loop, which is less than the accident analysis assumption of 0.35 gpm included in Section 15.1.5 of the Vogtle Units 1 and 2 FSAR.

Based on the information summarized above, the H* depths would be considered to be the minimum distance to be necessary to assure compliance with the structural requirements for the SGs. In addition, based on the results from consideration of application of the bellwether principle regarding potential leakage during postulated accident conditions, the planned alternate repair criterion/inspection length of 17 inches below the top of the tubesheet is conservative and justified.

The selection of the depth of 17 inches obviates the need to consider the location of the tube expansion transition below the top of the tubesheet, usually bounded by a length of 0.3 inches. For structural purposes, the value of 17 inches greatly exceeds the engagement lengths determined from the H* analysis included in Appendix A of this report. The application of the bellwether approach to the leak rate analysis as described in Section 6.0 of this report negates the need to consider specific distances from the top of the tubesheet and it relies on the relative magnitude of the joint contact pressure in the vicinity of the tube above 17 inches from the top of the tubesheet.

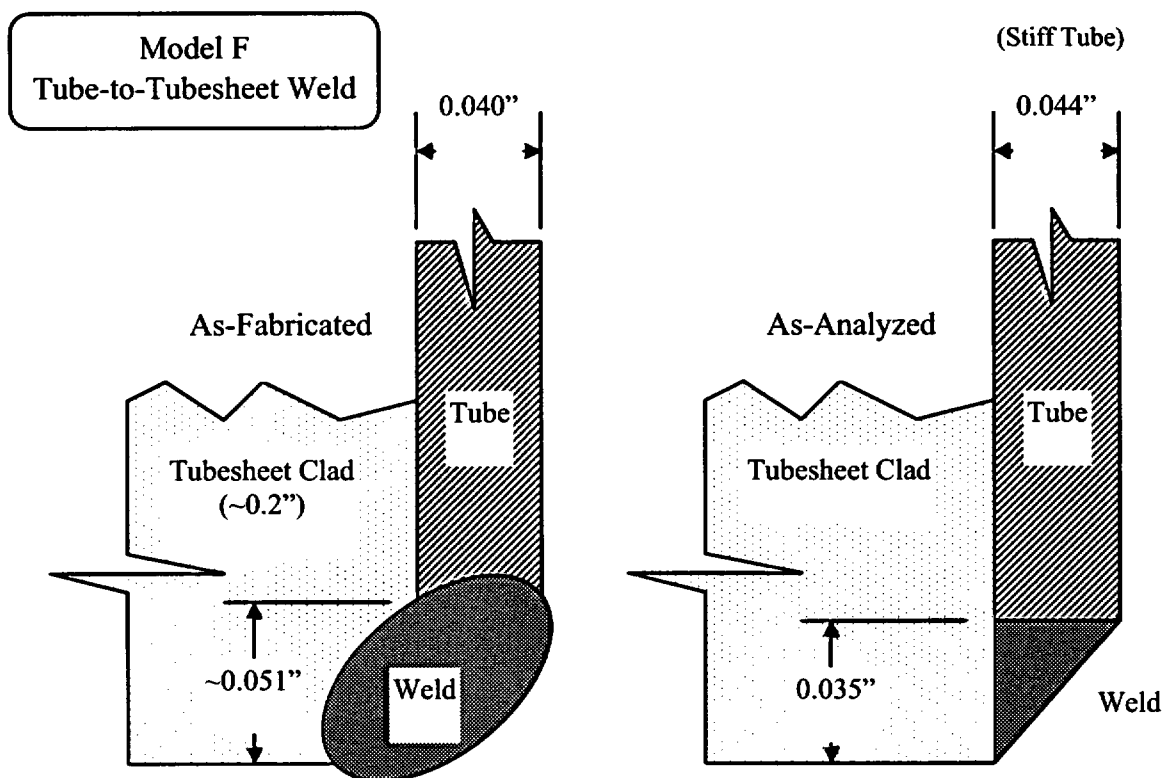


Figure 2-1. As-Fabricated & As-Analyzed Tube-to-Tubesheet Welds

3.0 Historical Background Regarding Tube Indications in the Tubesheet

There has been extensive experience associated with the operation of SGs wherein it was believed, based on NDE, that throughwall tube indications were present within the tubesheet. The installation of the SG tubes usually involves the development of a short interference fit, referred to as the tack expansion, at the bottom of the tubesheet. The tack expansion was usually effected by a hard rolling process through October of 1979 and thereafter, in most instances, by the Poisson expansion of a urethane plug inserted into the tube end and compressed in the axial direction. The rolling process by its very nature is considered to be more intensive with regard to metalworking at the inside surface of the tube and would be expected to lead to higher residual surface stresses. The manufacturing procedures and drawing requirements indicate that the urethane expansion process was used during fabrication of the Vogtle 1 & 2 SGs. The tube-to-tubesheet weld was then performed to create the ASME Code pressure boundary between the tube and the tubesheet.²

The development of the F* alternate repair criterion (ARC) in 1985-1986 for tubes hard rolled into the tubesheet was prompted by the desire to account for the inherent strength of the as-fabricated tube-to-tubesheet joint away from the weld and to allow tubes with degradation within the tubesheet to remain in service, Reference 16. The result of the development activity was the demonstration that the tube-to-tubesheet weld was superfluous with regard to the structural and leakage integrity of the rolled joint between the tube and the tubesheet. Once the plants were in operation, the structural and leakage resistance requirements for the joints were based on the plant Technical Specifications, and a means of demonstrating joint integrity that was acceptable to the NRC staff was delineated in Reference 17. License amendments were sought and granted for several plants with hard rolled tube-to-tubesheet joints to omit the inspection of the tube below a depth of about 1.5 inches from the top of the tubesheet. Similar criteria, designated as W*, were developed for explosively expanded tube-to-tubesheet joints in Westinghouse designed SGs in the 1991-1992 timeframe, Reference 18. The W* criteria were first applied to operating SGs in 1999 based on a generic evaluation for Model 51 SGs, Reference 19, and the subsequent safety evaluation by the NRC staff, Reference 20. However, the required engagement length to meet structural and leakage requirements was on the order of 4 to 6 inches because an explosively expanded joint does not have the same level of residual interference fit as that of a rolled joint. It is noted that the length of joint necessary to meet the structural performance criteria is not the same as, and is usually shorter than, that needed to meet the leakage integrity requirements.

The post-weld expansion of the tube into the tubesheet in the Vogtle 1 & 2 SGs was effected by a hydraulic expansion of the tube instead of rolling or explosive expansion. The hydraulically formed joints do not exhibit the level of interference fit that is present in rolled or explosively expanded joints; however, when the thermal and internal pressure expansion of the tube is considered during normal operation and postulated accident conditions, appropriate conclusions regarding the need for the weld similar to those for the other two types of joint can be made. Evaluations were performed in 1996 and 1997 of the effect of tube-to-tubesheet weld damage that occurred from an object in the bowl of SG 4 at Vogtle Unit 1, References 21 and 22 respectively. It was concluded in that evaluation that the strength of the tube-to-tubesheet joint is sufficient to

² The actual weld is between the Alloy 600 tube and weld buttering, a.k.a. cladding, on the bottom of the carbon steel tubesheet.

prevent pullout in accordance with the requirements of the performance criteria of Reference 10 and that a significant number of tubes could be damaged without violating the performance criterion related to the primary-to-secondary leak rate during postulated accident conditions. Both documents noted that the leak rate during normal operation would likely bound that to be expected during postulated accident conditions. A similar evaluation was performed for SG D at the Wolf Creek Generating Station with similar conclusions, Reference 23.

4.0 Design Requirements for the Tube-to-Tubesheet Joint Region

This section provides a review of the applicable design and analysis requirements, including the ASME Code pre-service design requirements of Section III and the operational/maintenance requirements of Section XI. The following is the Westinghouse interpretation of the applicable analysis requirements and criteria for the condition of TEW cracking. Recommendations that include code requirements and the USNRC and NEI positions are expressed in References 6 and 10 respectively. Reference 6 notes that:

"In accordance with Section III of the Code, the original design basis pressure boundary for the tube-to-tubesheet joint included the tube and tubesheet extending down to and including the tube-to-tubesheet weld. The criteria of Section III of the ASME Code constitute the "method of evaluation" for the design basis. These criteria provide a sufficient basis for evaluating the structural and leakage integrity of the original design basis joint. However, the criteria of Section III do not provide a sufficient basis by themselves for evaluating the structural and leakage integrity of a mechanical expansion joint consisting of a tube expanded against the tubesheet over some minimum embedment distance. If a licensee is redefining the design basis pressure boundary and is using a different method of evaluation to demonstrate the structural and leakage integrity of the revised pressure boundary, an analysis under 10 CFR 50.59 would determine whether a license amendment is required."

The industry definition of Steam Generator tubing excludes the tube-end weld from the pressure boundary as noted in NEI 97-06 (Reference 10):

"Steam generator tubing refers to the entire length of the tube, including the tube wall and any repairs to it, between the tube-to-tube sheet weld at the tube inlet and the tube-to-tube sheet weld at the tube outlet. The tube-to-tube sheet weld is not considered part of the tube."

The NRC has indicated its concurrence with this definition, see Reference 11 for example. In summary, from a non-technical viewpoint, no specific inspection of the tube-end welds would be required because:

1. The industry definition of the tube excludes the tube-end weld,
2. The ASME Code defers the judgment regarding the redefined pressure boundary to the licensing authority under 10CFR50.59,
3. The NRC has accepted this definition; therefore, by inference, may not consider cracked welds to be a safety issue on a level with that of cracked tubes, and
4. There is no qualified technique that can realistically be applied to determine if the tube-end welds are cracked.

However, based on the discussion of Information Notice 2005-09, Reference 2, it is clear that the NRC staff has concluded that "the findings at Catawba illustrate the importance of inspecting the

parent tube adjacent to the weld and the weld itself for degradation.” The technical considerations documented herein obviate the need for consideration of any and all non-technical arguments.

5.0 Structural Analysis of Tube-to-Tubesheet Joint

This section summarizes the structural aspects and analysis of the entire tube-to-tubesheet joint region. The tube end weld was originally designed as a pressure boundary structural element in accordance with the requirements of Section III of the ASME (American Society of Mechanical Engineers) Boiler and Pressure Vessel Code, Reference 5. The design and construction code for the Vogtle 1 & 2 SGs was the 1971 edition with the Summer 1972 addenda. This means that there were no strength considerations made with regard to the expansion joint between the tube and the tubesheet, including the tack expansion regardless of whether it was achieved by rolling or Poisson expansion of a urethane plug.

An extensive empirical and analytical evaluation of the structural capability of the as-installed tube-to-tubesheet joints based on considering the weld to be absent was performed specifically for the Vogtle 1 & 2 Model F SGs and the results are reported below. Typical Model F hydraulic expansion joints with lengths comparable to those being proposed in what follows for limiting specialized probe examination were tested for pullout resistance strength at temperatures ranging from 70 to 600°F. The results of the tests coupled with those from finite element evaluations of the effects of temperature and primary-to-secondary pressure on the tube-to-tubesheet interface loads have been used to determine the engagement lengths that would be sufficient to equilibrate the axial loads resulting from consideration of 3 times the normal operating and 1.4 times the limiting accident condition pressure differences. Variation in required engagement length is a function of tube location, i.e., row and column, and decreases away from the center of the SG where the maximum value applies. The tubesheet bows, i.e., deforms, upward from the primary-to-secondary pressure difference and results in the tube holes becoming dilated above the neutral plane of the tubesheet, which is a little below the mid-plane because of the effect of the tensile membrane stress from the pressure loading. The amount of dilation is a maximum very near the radial center of the tubesheet (restricted by the divider plate) and diminishes with increasing radius outward. Moreover, the tube-to-tubesheet joint becomes tighter below the neutral axis and is a maximum at the bottom of the tubesheet³. In conclusion, the need for the weld is obviated by the interference fit between the tube and the tubesheet. Axial loads are not transmitted to the portion of the tube below the H* distance during operation or faulted conditions, by factors of safety of at least 3 and 1.4 respectively, including postulated loss of coolant accidents (LOCA), and inspection of the tube below the H* distance including the tube-to-tubesheet weld is not technically necessary. Also, even if the expansion joint were not present, there would be no effect on the strength of the weld from axial cracks, and tubes with circumferential cracks up to about 180° by 100% deep would have sufficient strength to meet the nominal ASME Code structural requirements, based on the margins of safety reported in Reference 12.

An examination of Table A-6 through Table A-10 illustrates that the holding strength of the tube-to-tubesheet joint in the vicinity of a depth of 17 inches is much greater than at the top of the tubesheet in the range of H* as listed in Table A-12. The radii reported in these tables were picked to conservatively represent the entire radial zones of consideration as defined on Figure A-1. For example, Zone C has a maximum radius of 30.2 inches. However, in order to establish H* values

³ There is a small reversal of the bending stress beyond a radius of about 55 inches because the support ring restricts rotation and the hole dilation is at the bottom of the tubesheet.

that were conservative throughout the zone, the tube location for which the analysis results were most severe above the neutral axis were reported, i.e., those values calculated for a tube at a radius of 4.02 inches. The values are everywhere conservative above the neutral surface of the tubesheet for tubes in Zone C. Likewise for tubes in Zone B under the heading 48.61 inches where the basis for the calculation was a tube at a radius of 30.19 inches. To illustrate the extreme conservatism associated with the holding strength of the joint at and below the neutral surface of the tubesheet, and to identify the proper tube radii for consideration the following is noted:

- In the center of the tubesheet the incremental holding strength in the 2.5 inch range from 8 to 10.5 inches below the top of the tubesheet during NOp is about 940 lbf per inch using a coefficient of friction of 0.2. The performance criterion for $3 \cdot \Delta P$ is roughly met by the first 1.8 inches of engagement above the lower elevation. At a radius of 58 inches the corresponding length of engagement needed is about 1.7 inches.
- The corresponding values for steam line break conditions are 1.25 and 1.15 inches at radii of 4.02 and 58.3 inches respectively. In other words, while a value of 7.0 inches was determined for H^* from the top of the tubesheet, a length of 1.15 to 1.25 inches would be sufficient at the middle of the tubesheet.
- At a depth of 17 inches, engagement lengths of less than 1.8 inches are needed to resist the pullout force associated with a differential pressure of $3 \Delta P$ for normal operation and less than 1.15 inches for SLB conditions. The latter value applies to peripheral locations where the joint is actually tighter near the mid-plane than at the bottom. At central locations the length of engagement needed to resist pullout is more on the order of less than 1.25 inches.

6.0 Leak Rate Analysis of Cracked Tube-to-Tubesheet Joints

This section of the report presents a discussion of the leak rate expectations from axial and circumferential cracking confined to the tube-to-tubesheet joint region, including the tack expansion region, the tube-to-tubesheet welds and areas where degradation could potentially occur, due to bulges and overexpansions for example, within the tube at a distance 17 inches from the top of the tubesheet. Although the welds are not part of the tube per the technical specifications, consideration is given in deference to the discussions of the NRC staff in Information Notice 2005-09 and Generic Letter 2004-01, and References 2 and 6 respectively. It is noted that the methods discussed below support a one cycle change to the Vogtle 1 & 2 Technical Specification. With regard to the inherent conservatism embodied in the application of any predictive methods it is noted that the presence of cracking was not confirmed because removal of a tube section was not performed at Catawba 2 or Vogtle 1.

From an engineering expectation standpoint, if there is no meaningful primary-to-secondary leakage during normal operation, there should likewise be no meaningful leakage during postulated accident conditions from indications located approximately below the mid-plane of the tubesheet. The rationale for this is based on consideration of the deflection of the tubesheet with attendant dilation and diminution (expansion and contraction) of the tubesheet holes. In effect, the leakage flow area depends on the contact pressure between the tube and tubesheet and would be expected to decrease during postulated accident conditions below some distance from the top of the tubesheet. The primary-to-secondary pressure difference during normal operation is on the order of 1200 to 1400 psi, while that during a postulated accident, e.g., steam line and feed line break, is on the order of 2560 to 2650 psi.⁴ Above the neutral plane of the tubesheet the tube holes tend to experience a dilation due to pressure induced bow of the tubesheet. This means that the contact pressure between the tubes and the tubesheet would diminish above the neutral plane in the central region of the tubesheet at the same time as the driving potential would increase. Therefore, if there was leakage through the tube-to-tubesheet crevice during normal operation from a through-wall tube indication, that leak rate could be expected to increase during postulated accident conditions. Based on early NRC staff queries regarding the leak rate modeling code associated with calculating the expected leak rate, it was expected that efforts to license criteria based on estimating the actual leak rate as a function of the contact pressure during faulted conditions on a generic basis would be problematic.

As noted, the tube holes diminish in size below the neutral plane of the tubesheet because of the upward bending and the contact pressure between the tube and the tubesheet increases. When the differential pressure increases during a postulated faulted event the increased bow of the tubesheet leads to an increase in the tube-to-tubesheet contact pressure, increasing the resistance to flow. Thus, while the dilation of the tube holes above the neutral plane of the tubesheet presents additional analytic problems in estimating the leak rate for indications above the neutral plane, the diminution of the holes below the neutral plane presents definitive statements to be made with regard to the trend of the leak rate, hence, the bellwether principle. Independent consideration of the effect of the tube-to-tubesheet contact pressure leads to similar conclusions with regard to the

⁴ The differential pressure could be on the order of 2405 psi if it is demonstrated that the power operated relief valves will be functional.

opening area of the cracks in the tubes, thus further restricting the leak rate beyond that through the interface between the tube and the tubesheet.

In order to accept the concept of normal operation being a bellwether for the postulated accident leak rate for indications above the neutral plane of the tubesheet, the change in leak rate had to be quantified using a somewhat complex, physically sound model of the thermal-hydraulics of the leak rate phenomenon. This is not necessarily the case for cracks considered to be present below the neutral plane of the tubesheet. This is because a diminution of the holes takes place during postulated accident conditions below the neutral plane relative to normal operation. For example, at a radius of a little more than 30 inches from the center of the SG and 10.5 inches from the TTS, the contact pressure during normal operation is calculated to be about 1072 to 1139 psi⁵, see the third contact pressure column in Table A-6 and Table A-7, respectively, while the contact pressure during a postulated SLB would be on the order of 1670 psi, Table A-8, and during a postulated FLB would be on the order of 2029 to 2075 psi at the bottom of the tubesheet, Table A-9 and Table A-10, respectively.

Note: The radii specified in the heading of the tables are the maximum values for the respective zones analyzed, hence the contact pressures in the center column correspond to the radius specified for the left column, etc. The leftmost column lists the contact pressure values for a radius of 4.02 inches, but is used to a radius of 12 inches, etc. Also, the values tabulated do not include the calculated residual preload from the tube installation, which is not necessary for this comparison.

The analytical model for the flow through the crevice, the Darcy equation for flow through porous media, indicates that flow would be expected to be proportional to the differential pressure. Thus, a doubling of the leak rate could be predicted if the change in contact pressure between the tube and the tubesheet were ignored. Examination of the nominal correlation on Figure 6-1 indicates that the crevice resistance to flow per unit length (the loss coefficient) would increase during a postulated SLB event.

The leak rate from a crack located within the tubesheet is governed by the crack opening area, the resistance to flow through the crack, and the resistance to flow provided by the tube-to-tubesheet joint. The path through the tube-to-tubesheet joint is also frequently referred to as a crevice, but is not to be confused with the crevice left at the top of the tubesheet from the expansion process. The presence of the joint makes the flow from cracks within the tubesheet much different from the flow to be expected from cracks outside of the tubesheet. The tubesheet prevents outward deflection of the flanks of cracks, a more significant effect for axial than for circumferential cracks, which is a significant contributor to the opening area presented to the flow. In addition, the restriction provided by the tubesheet greatly restrains crack opening in the direction perpendicular to the flanks regardless of the orientation of the cracks. The net effect is a large, almost complete restriction of the leak rate when the tube cracks are within the tubesheet.

The leak path through the crack and the crevice is very tortuous. The flow must go through many turns within the crack in order to pass through the tube wall, even though the tube wall thickness is relatively small. The flow within the crevice must constantly change direction in order to follow a

⁵ The column headed 48.61 inches includes the range of $30 < R \leq 48.61$ inches.

path that is formed between the points of hard contact between the tube and the tubesheet as a result of the differential thermal expansion and the internal pressure in the tube. It is likely that there is both mechanical dispersion and molecular diffusion taking place. The net result is that the flow is best described as primary-to-secondary weepage. At its base, the expression used to predict the leak rate from tube cracks through the tube-to-tubesheet crevice is the Darcy expression for flow rate, Q , through porous media, i.e.,

$$Q = \frac{1}{K \mu} \frac{dP}{dz} \quad (6-1)$$

where μ is the viscosity of the fluid, P is the driving pressure, z is the physical dimension in the direction of the flow, and K is the "loss coefficient" which can also be termed the flow resistance if the other terms are taken together as the driving potential. The loss coefficient is found from a series of experimental tests involving the geometry of the particular tube-to-tubesheet crevice being analyzed, including factors such as surface finish, and then applied to the cracked tube situation.

If the leak rate during normal operation was 0.10 gpm (about 150 gpd), the postulated accident condition leak rate would be on the order of 0.20 gpm if only the change in differential pressure were considered; however, the estimate would be reduced if the increase in contact pressure between the tube and the tubesheet were to be included during a postulated steam line break event. An examination of the contact pressures as a function of depth in the tubesheet from the finite element analyses of the tubesheet as reported in Table A-6 through Table A-10 shows that the bellwether principle applies to a significant extent to all indications below the neutral plane of the tubesheet, and may apply to somewhat higher elevations. At the central plane of the tubesheet, the increase in contact pressure shown on Figure 6-5 is more on the order of 500 to 600 psi relative to that during NOp for all tubes regardless of radius. Still, the fact that the contact pressure increases means that the SLB leak rate would be expected to be bounded by no more than a factor of two relative to normal operation. The flow resistance would be expected to increase at a rate greater than that of the contact pressure and the increase in driving pressure would be mostly offset by the increase in the resistance of the joint.

The numerical results from the finite element analyses are presented on Figure 6-2 at the bottom of the tubesheet. A comparison of the contact pressure during postulated SLB conditions relative to that during NOp is also provided for depths of 16.9, 12.6, 10.5, 8.25, and 6.0 inches below the top of the tubesheet. The observations are discussed in what follows:

- Near the bottom of the tubesheet, Figure 6-2, the contact pressure increases by 1712 psi near the center of the tubesheet, exhibits no change at a radius of about 55 inches, and diminishes by 416 psi at the extreme periphery, a little less than 60 inches from the center.
- At 16.9 inches below the top of the tubesheet (about 4.13 inches from the bottom of the tubesheet) the contact pressure increases by about 1276 psi at the center to a minimum of about 336 psi at a radius of 56 inches, Figure 6-3. The contact pressure during a SLB is everywhere greater than that during NOp. The influence of the channelhead and shell at the periphery causes the deformation to become non-uniform near the periphery.

-
- At a depth of 12.6 inches, Figure 6-4, the contact pressure increase ranges from a maximum of 724 psi near the center of the tubesheet to 561 psi at a radius of almost 52 inches as shown on Figure 6-4.
 - At roughly the neutral surface, about 10.5 inches, Figure 6-5, the contact pressure during SLB is uniformly greater than that during normal operation by about 550 psi (ranging from 531 to 636 psi traversing outward).
 - At a depth of 8.25 inches from the TTS, Figure 6-6, the contact pressure increases by about 281 psi near the center of the TS to a maximum increase of 640 psi near the periphery.
 - At a depth of about 6 inches from the TTS, Figure 6-7, the contact pressure increases by about 19 psi at the center of the TS, i.e., is nearly invariant, and increases by 629 psi near the periphery.
 - Although not depicted, the contact pressure at a depth of 4 inches decreases by 225 psi at 6 inches from the center of the tubesheet, exhibits no change at a radius of 28 inches, and increases by about 620 psi at a radius of 58 inches.

The leak rate from any indication is determined by the total resistance of the crevice from the elevation of the indication to the top of the tubesheet in series with the resistance of the crack itself, which is also expected to increase with contact pressure (The effect of hoop compression on axial cracks would overwhelm the effect of the fluid pressure on the flanks.). A comparison of the curves on Figure 6-7 relative to those on Figure 6-5 indicates that the contact pressure generally increases for a length of at least 4 inches upward from the mid-plane for all tubes.

The trend is consistent, at radii where the contact pressure decreases or the increase is not as great near the bottom of the tubesheet, the increase at higher elevations would be expected to compensate. For example, the contact pressures on Figure 6-2 near the bottom of the tubesheet show a decrease beyond a radius of 55 inches; however, the increase at 8.4 inches above the bottom, Figure 6-3 is significant. For the outboard tubes the increase in contact pressure extends all the way to the top of the tubesheet.

A comparison of the curves at the various elevations leads to the conclusion that for a length of 11 inches upward from an elevation of about 4.1 inches from the bottom of the tubesheet, there is always an increase in the contact pressure in going from normal operation conditions to postulated SLB conditions. At a depth 6.0 inches, the information on Figure 6-7 indicates the contact pressure is the same at the worst location, while Figure 6-3 illustrates that the SLB contact pressure is everywhere greater at a depth of 16.9 inches. Hence, it is reasonable by inspection to expect that omission of the examination of bulges or other artifacts below a depth of 6 inches from the top of the tubesheet would lead to a high level of confidence that the potential leak rate from indications below the lower bound inspection elevation during a postulated SLB event will be bounded by twice the normal operation primary-to-secondary leak rate. The reason that 6 inches cannot be used is that although the contact pressure is no less than the same at that depth, the integrated contact pressure must be used to obtain the total resistance and the contact pressure above 6 inches depth decreases during the SLB event.

Noting that the number of tubes populating the tubesheet increases with the square of the radius, the number of tubes for which the contact pressure is greater during a SLB than during NOp at the H* depth from the TTS is far greater than the number for which the contact pressure decreases, i.e., 96% of the tubes are at a radius greater than 12 inches from the center of the tubesheet.



Figure 6-1. Loss Coefficient Values for Model F Leak Rate Analysis

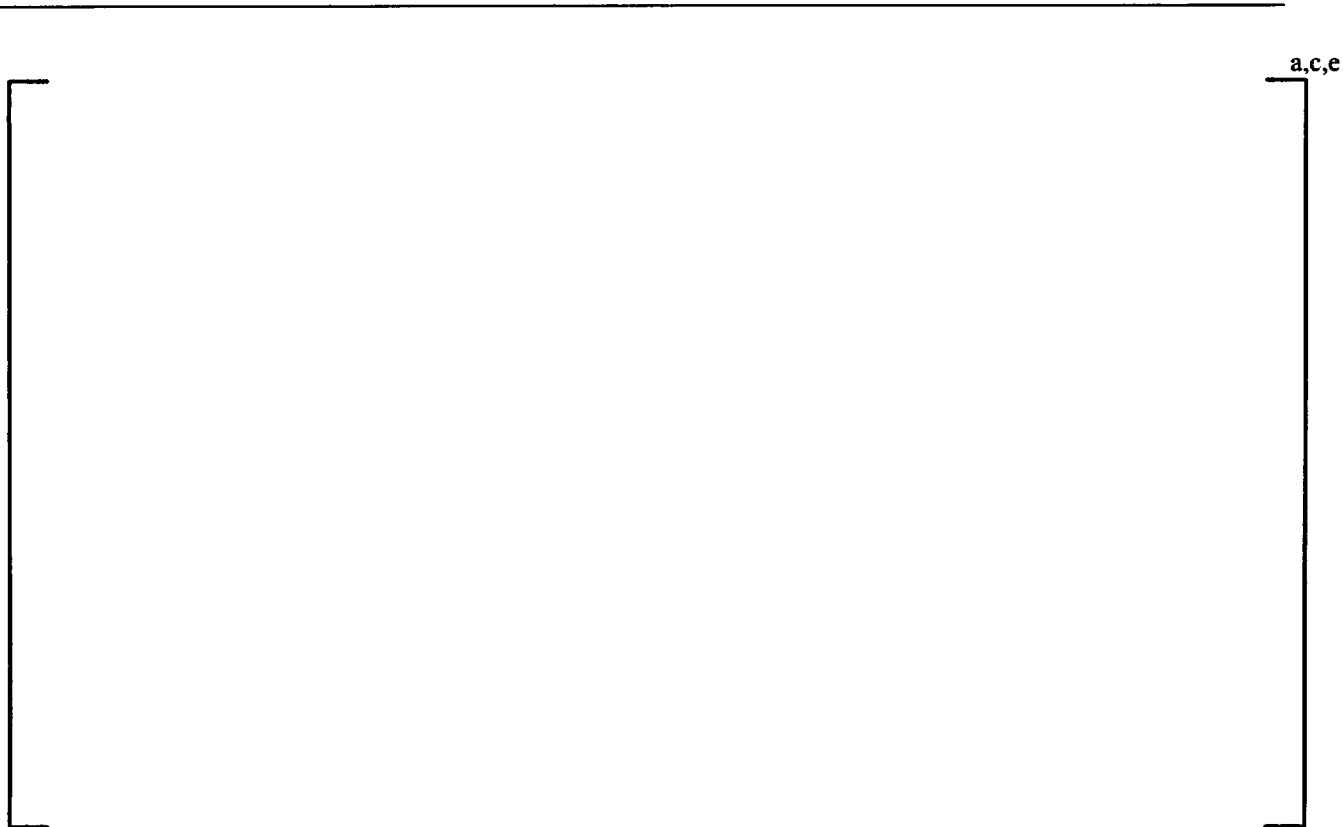


Figure 6-2. Change in Contact Pressure at 20.0 inches Below the TTS



Figure 6-3. Change in Contact Pressure at 16.9 inches Below the TTS



Figure 6-4. Change in contact pressure at 12.6 inches below the TTS



Figure 6-5. Change in contact pressure at 10.5 inches below the TTS



Figure 6-6. Change in contact pressure at 8.25 inches below the TTS



Figure 6-7. Change in contact pressure at 6.0 inches below the TTS

7.0 Conclusions

The evaluation of Section 5.0 of this report provides a technical basis for assuring that the structural performance criteria of NEI 97-06 are inherently met for degradation of any extent below the H* depth identified in Table A-12, i.e., depths ranging from 2.3 to 7.0 inches below the TTS (including allowance of 0.3 inches to account for the hydraulic expansion transition) selected to be bounding for all tubes in all zones. The corresponding evaluation presented in Section 6.0 provides a technical basis for bounding the potential leak rate from non-detected indications in the tube region below 17 inches from the top of the tubesheet as no more than twice the leak rate during normal operation. The conclusions also apply to any postulated indications in the tack expansion region and in the tube-to-tubesheet welds, although the level of conservatism would be significantly more. As noted in the introduction to this report, the reporting of crack-like indications in the tube-to-tubesheet welds would be expected to occur inadvertently since no structural or leak rate technical reason exists for a specific examination to take place.

The conclusions to be drawn from the performed analyses are that:

- 1) There is no structural integrity concern associated with tube or tube weld cracking of any extent provided it occurs below the H* distance as reported in Section 5.0 of this report. The pullout resistance of the tubes has been demonstrated for axial forces associated with 3 times the normal operating differential pressure and 1.4 times differential pressure associated with the most severe postulated accident.
- 2) Contact forces during postulated LOCA events are sufficient to resist axial motion of the tube. Also, if the tube end welds are not circumferentially cracked, the resistance of the tube-to-tubesheet hydraulic joint is not necessary to resist push-out. Moreover, the geometry of any postulated circumferential cracking of the weld would result in a configuration that would resist pushout in the event of a loss of coolant accident. In other words, the crack flanks would not form the cylindrical surface necessary such that there would be no resistance to expulsion of the tube in the downward direction.
- 3) The SLB leak rate for indications below the depth of 17 inches from the top of the tubesheet would be bounded by twice the leak rate that is present during normal operation of the plant regardless of tube location in the bundle. This is initially apparent from comparison of the contact pressures from the finite element analyses over the full range of radii from the center of the tubesheet, and ignores any increase in the leak rate resistance due to the contact pressure changes and associated tightening of the crack flanks.

In conclusion, a relocation of the pressure boundary to 17 inches from the top of the tubesheet is acceptable from both structural and leak rate considerations depending on the relative allowable leak rate during accident conditions. The prior conclusions rely on the inherent strength and leak rate resistance of the hydraulically expanded tube-to-tubesheet joint, a feature which was not considered or permitted to be considered for the original design of the SG. Thus, omission of the inspection of the weld constitutes a reassignment of the pressure boundary to the tube-to-tubesheet interface. Similar considerations for tube indications require NRC staff approval of a license amendment.

The analyses demonstrate that the evaluation of the conditions on the hot leg bound those for the cold leg with regard to leak rate performance. However, as previously noted, the structural results for the cold leg are bounding relative to the hot leg. The difference is approximately 0.3 inch. A summary is provided in Table A-12.

With regards to the preparation of a significant hazards determination, the results of the testing and analyses demonstrate that the relocation of the pressure boundary to a depth below 17 inches from the top of the tubesheet does not lead to an increase in the probability or consequences of the postulated limiting accident conditions because the margins inherent in the original design basis are maintained and the expected leak rate during the postulated accident is not expected to increase beyond the plant specific limit. In addition, the relocation of the pressure boundary does not create the potential for a new or departure from the previously evaluated accident events. Finally, since the margins inherent in the original design bases are maintained, no significant reduction in the margin of safety would be expected.

8.0 References

1. OE19662 (Restricted & Confidential), "Steam Generators (Catawba Nuclear Power Station)," Institute of Nuclear Power Operations (INPO), Atlanta, GA, USA, December 13, 2004.
2. IN 2005-09, "Indications in Thermally Treated Alloy 600 Steam Generator Tubes and Tube-to-Tubesheet Welds," United States Nuclear Regulatory Commission, Washington, DC, April 7, 2005.
3. SGMP-IL-05-01, "Catawba Unit 2 Tubesheet Degradation Issues," EPRI, Palo Alto, CA, March 4, 2005.
4. OE20339, "Vogtle Unit 1 Steam Generator Tube Crack Indications," Institute of Nuclear Power Operations (INPO), Atlanta, GA, USA, April 4, 2005.
5. ASME Boiler and Pressure Vessel Code, Section III, "Nuclear Power Plant Components," American Society of Mechanical Engineers, New York, New York, 1971, Summer 1972 Addenda.
6. GL 2004-01, "Requirements for Steam Generator Tube Inspections," United States Nuclear Regulatory Commission, Washington, DC, August 30, 2004.
7. NRC Letter, "Wolf Creek Generating Station – Issuance of Exigent Amendment Re: Steam Generator (SG) Tube Surveillance Program (TAC No. MC6757)," United States Nuclear Regulatory Commission, Washington, DC, April 28, 2005.
8. NRC Letter, "Braidwood Station, Units 1 and 2 – Issuance of Exigent Amendments Re: Revision of Scope of Steam Generator Inspections for Unit 2 Refueling Outage 11 – (TAC Nos. MC6686 and MC6687)," United States Nuclear Regulatory Commission, Washington, DC, April 25, 2005.
9. NRC Letter, "Vogtle Electric Generating Plant, Units 1 and 2 RE: Issuance of Amendments Regarding the Steam Generator Tube Surveillance Program (TAC Nos. MC8078 and MC8079)," United States Nuclear Regulatory Commission, Washington, DC, September 21, 2005.
10. NEI 97-06, Rev. 2, "Steam Generator Program Guidelines," Nuclear Energy Institute, Washington, DC, May 2005 (issued for use by NEI on September 2, 2005 and confirmed by the NRC staff as complying with TSTF-449 on October 3, 2005). Implementation is mandatory by March 2, 2006.
11. Federal Register, Part III, Nuclear Regulatory Commission, National Archives and Records Administration, Washington, DC, pp. 10298 to 10312, March 2, 2005.
12. WNET-180 (Proprietary), Volume 11, "Model F Steam Generator Stress Report," Westinghouse Electric Company LLC, Pittsburgh, PA, September 1980.
13. NPD/E/PEN-99-255, "Applicable ASME Codes for the Original and Replacement Steam Generators," Westinghouse Electric Company LLC, Pittsburgh, PA, June 29, 1999.

-
14. ASME Boiler and Pressure Vessel Code, Section XI, "Rules for Inservice Inspection of Nuclear Power Plant Components," American Society of Mechanical Engineers, New York, New York, 1971.
 15. ASME Boiler and Pressure Vessel Code, Section XI, "Rules for Inservice Inspection of Nuclear Power Plant Components," American Society of Mechanical Engineers, New York, New York, 2004.
 16. WCAP-11224, Rev. 1, "Tubesheet Region Plugging Criterion for the Duke Power Company McGuire Nuclear Station Units 1 and 2 Steam Generators," Westinghouse Electric Company LLC, Pittsburgh, PA, October 1986.
 17. RG 1.121 (Draft), "Bases for Plugging Degraded PWR Steam Generator Tubes," United States Nuclear Regulatory Commission, Washington, DC, August 1976.
 18. WCAP-13532, Rev. 1, "Sequoyah Units 1 and 2 W* Tube Plugging Criteria for SG Tubesheet Region of WEXTEx Expansions," Westinghouse Electric Company LLC, Pittsburgh, PA, 1992.
 19. WCAP-14797, "Generic W* Tube Plugging Criteria for 51 Series Steam Generator Tubesheet Region WEXTEx Expansions," Westinghouse Electric Company LLC, Pittsburgh, PA, 1997.
 20. "Safety Evaluation by the Office of Nuclear Reactor Regulation Related to Amendment No. 129 to Facility Operating License No. DPR-80 and Amendment No. 127 to Facility Operating License No. DPR-82 Pacific Gas and Electric Company Diablo Canyon Nuclear Power Plant, Units 1 and 2 Docket Nos. 50-275 and 50-323," United States Nuclear Regulatory Commission, Washington, DC, 1999.
 21. NSD-RFK-96-015, "Vogtle 1 Tube Integrity Evaluation, Loose Part Affected SG," Westinghouse Electric Company LLC, Pittsburgh, PA, June 9, 1996.
 22. WCAP-14871 (Proprietary), "Vogtle Electric Generating Plant (VEGP) Steam Generator Tube-to-Tubesheet Joint Evaluation," Westinghouse Electric Company LLC, Pittsburgh, PA, May 1997.
 23. LTR-SGDA-02-162 (Proprietary), Revision 1, "Bounding Evaluation for Operation of Wolf Creek Nuclear Operating Corporation Steam Generator D with Impacted Channelhead Components," Westinghouse Electric Company LLC, Pittsburgh, PA, November 2003.

Appendix A – Structural Analysis of the Tube-to Tubesheet Joint

A.1 Evaluation of Tubesheet Deflection Effects for Tube-to-Tubesheet Contact Pressure

A finite element model was developed for the Model F tubesheet, channel head, and shell region to determine the tubesheet hole dilations in the Vogtle 1 & 2 SGs. [

] ^{a,c,e} loads in the
tube.

A.1.1 Material Properties and Tubesheet Equivalent Properties

The tubes in the Vogtle 1 & 2 SGs were fabricated of A600TT material. Summaries of the applicable mechanical and thermal properties for the tube material are provided in Table A-1. The tubesheets were fabricated from SA-508, Class 2a, material for which the properties are listed in Table A-2. The shell material is SA-533 Grade A Class 2, and its properties are in Table A-3. Finally, the channel head material is SA-216 Grade WCC, and its properties are in Table A-4. The material properties were obtained from the ASME B&PV (Boiler and Pressure Vessel) Code, Reference A.2.

The perforated tubesheet in the Model F channel head assembly is treated as an equivalent solid plate in the global finite element analysis. An accurate model of the overall plate behavior was achieved by using the concept of an equivalent elastic material with anisotropic properties. For square tubesheet hole patterns, the equivalent material properties depend on the orientation of loading with respect to the symmetry axes of the pattern. An accurate approximation was developed in Reference A.3, where energy principles were used to derive effective average isotropic elasticity matrix coefficients for the in-plane loading. The average isotropic stiffness formulation gives results that are consistent with those using the Minimum Potential Energy Theorem, and the elasticity problem thus becomes axisymmetric. The solution for strains is sufficiently accurate for design purposes, except in the case of very small ligament efficiencies, which are not of issue for the evaluation of the SG tubesheet.

The stress-strain relations for the axisymmetric perforated part of the tubesheet are given by:

$$\begin{bmatrix} \dot{\sigma}_R \\ \dot{\sigma}_\theta \\ \dot{\sigma}_Z \\ \dot{\tau}_{RZ} \end{bmatrix} = \begin{bmatrix} D_{11} & D_{12} & D_{13} & 0 \\ D_{21} & D_{22} & D_{23} & 0 \\ D_{31} & D_{32} & D_{33} & 0 \\ 0 & 0 & 0 & D_{44} \end{bmatrix} \begin{bmatrix} \dot{\epsilon}_R \\ \dot{\epsilon}_\theta \\ \dot{\epsilon}_Z \\ \dot{\gamma}_{RZ} \end{bmatrix}$$

with the elasticity coefficients are calculated as:

$$D_{11} = D_{22} = \frac{\bar{E}_p^*}{f(1 + \bar{\nu}_p^*)} \left[1 - \frac{\bar{E}_p^*}{E_z^*} \nu^2 \right] + \frac{1}{2} \left[\bar{G}_p^* - \frac{\bar{E}_p^*}{2(1 + \bar{\nu}_p^*)} \right]$$

$$D_{21} = D_{12} = \frac{\bar{E}_p^*}{f(1 + \bar{\nu}_p^*)} \left[\bar{\nu}_p^* + \frac{\bar{E}_p^*}{E_z^*} \nu^2 \right] - \frac{1}{2} \left[\bar{G}_p^* - \frac{\bar{E}_p^*}{2(1 + \bar{\nu}_p^*)} \right]$$

$$D_{13} = D_{23} = D_{31} = D_{32} = \frac{\bar{E}_p^* \nu}{f}$$

$$D_{33} = \frac{E_z^*(1 - \bar{\nu}_p^*)}{f} \text{ and } D_{44} = \bar{G}_z^*$$

$$\text{where } f = 1 - \bar{\nu}_p^* - 2 \frac{\bar{E}_p^*}{E_z^*} \nu^2 \text{ and } \bar{G}_p^* = \frac{\bar{E}_d^*}{2(1 + \bar{\nu}_d^*)}.$$

Here,

\bar{E}_p^* = Effective elastic modulus for in-plane loading in the pitch direction,

E_z^* = Effective elastic modulus for loading in the thickness direction,

$\bar{\nu}_p^*$ = Effective Poisson's ratio for in-plane loading in the pitch direction,

\bar{G}_p^* = Effective shear modulus for in-plane loading in the pitch direction,

\bar{G}_z^* = Effective modulus for transverse shear loading,

\bar{E}_d^* = Effective elastic modulus for in-plane loading in the diagonal direction,

$\bar{\nu}_d^*$ = Effective Poisson's ratio for in-plane loading in the diagonal direction, and,

ν = Poisson's ratio for the solid material.

The tubesheet is a thick plate and the application of the pressure load results in a generalized plane strain condition. The pitch of the square, perforated hole pattern is 0.98 inches and nominal hole diameters are 0.703 inch. The ID of the tube after expansion into the tubesheet is taken to be about 0.625 inch based on an approximation of 1% thinning during installation associated with constant material volume. Equivalent properties of the tubesheet are calculated without taking credit for the stiffening effect of the tubes.

$$\text{Ligament Efficiency, } \eta = \frac{h_{\text{nominal}}}{P_{\text{nominal}}}$$

where:

h_{nominal}	=	$P_{\text{nominal}} - d_{\text{maximum}}$
P_{nominal}	=	0.980 inches, the pitch of the square hole pattern
d_{maximum}	=	.706 inches, the tube hole diameter

Therefore, $h_{\text{nominal}} = 0.2745$ inches (0.980-0.706), and $\eta = 0.2796$ when the tubes are not included. From Slot, Reference A.4, the in-plane mechanical properties for Poisson's ratio of 0.3 are:

Property	Value
E_p^* / E	= 0.3977
ν_p^*	= 0.1630
E_d^* / E	= 0.2137
ν_d^*	= 0.5531
E^* / E	= 0.3057
ν^*	= 0.3580

where the subscripts p and d refer to the pitch and diagonal directions, respectively. These values are substituted into the expressions for the anisotropic elasticity coefficients given previously. In the global model, the X-axis corresponds to the radial direction, the Y-axis to the vertical or tubesheet thickness direction, and the Z-axis to the hoop direction. The directions assumed in the derivation of the elasticity coefficients were X- and Y-axes in the plane of the tubesheet and the Z-axis through the thickness. In addition, the order of the stress components in the WECAN/Plus (Reference A.5) elements used for the global model is σ_{xx} , σ_{yy} , τ_{xy} , and σ_{zz} . The mapping between the Reference A.3 equations and WECAN/+ is therefore:

Coordinate Mapping	
Reference A.3	WECAN/+
1	1
2	4
3	2
4	3

Table A-2 gives the modulus of elasticity, E, of the tubesheet material at various temperatures. Using the equivalent property ratios calculated above in the equations presented at the beginning of this section yields the elasticity coefficients for the equivalent solid plate in the perforated region of the tubesheet for the finite element model.

A.1.2 Finite Element Model

The analysis of the contact pressures utilizes conventional (thick shell equations) and finite element analysis techniques. A finite element analysis (FEA) model was developed for the Model F SG channel head/ tubesheet/ shell region in order to determine the tubesheet rotations. The elements used for the models of the channel head/ tubesheet/ shell region were the quadratic version of the 2-D axisymmetric isoparametric elements STIF53 and STIF56 of WECAN-Plus (Reference A.5). The model for the Model F SG is shown on Figure A-2.

The unit loads applied to this model are listed below:

Unit Load	Magnitude
Primary Side Pressure	1000 psi
Secondary Side Pressure	1000 psi
Tubesheet Thermal Expansion	500°F
Shell Thermal Expansion	500°F
Channel Head Thermal Expansion	500°F

The three temperature loadings consist of applying a uniform thermal expansion to each of the three component members, one at a time, while the other two remain at ambient conditions. The boundary conditions imposed for all five cases are: $UX = 0$ at all nodes on the centerline, and $UY = 0$ at one node on the lower surface of the tubesheet support ring. In addition, an end cap load was applied to the top of the secondary side shell for the secondary side pressure unit load equal to:

$$P_{endcap} = -\frac{R_i^2}{R_o^2 - R_i^2} P$$

where, R_i = Inside radius of secondary shell in finite element model = 64.69 in.

R_o = Outside radius of secondary shell in finite element model = 68.0 in.

P = Secondary pressure unit load = 1000 psi.

This procedure yielded displacements throughout the tubesheet for the unit loads.

A.1.3 Tubesheet Rotation Effects

Loads are imposed on the tube OD as a result of tubesheet rotations under pressure and temperature conditions. Previous calculations performed [

] ^{a,c,e}.

The radial deflection, UR , at any point within the tubesheet is found by scaling and combining the unit load radial deflections at that location according to:

$$\left[\begin{array}{c} \text{a,c,e} \end{array} \right]$$

This expression is used to determine the radial deflections along a line of nodes at a constant axial elevation (e.g., top of the tubesheet) within the perforated area of the tubesheet. The expansion of a hole of diameter D in the tubesheet at a radius R is given by:

$$\left[\begin{array}{c} \text{a,c,e} \\ \text{[]} \end{array} \right]$$

U_R is available directly from the finite element results. dU_R/dR may be obtained by numerical differentiation.

The maximum expansion of a hole in the tubesheet is in either the radial or circumferential direction. [

$$]^{a,c,c}$$

Where SF is a scale factor between zero and one. For the eccentricities typically encountered during tubesheet rotations, [$]^{a,c,c}$. These values are listed in the following table:

$$\left[\begin{array}{c} \text{a,c,c} \\ \text{[]} \end{array} \right]$$

The data were fit to the following polynomial equation:

$$\left[\begin{array}{c} \text{a,c,e} \\ \text{[]} \end{array} \right]$$

The hole expansion calculation as determined from the finite element results includes the effects of tubesheet rotations and deformations caused by the system pressures and temperatures. It does not include the local effects produced by the interactions between the tube and tubesheet hole. Standard thick shell equations, including accountability for the end cap axial loads in the tube

(Reference A.6), in combination with the hole expansions from above are used to calculate the contact pressures between the tube and the tubesheet.

The unrestrained radial expansion of the tube OD due to thermal expansion is calculated as:

$$\Delta R_t^{th} = c \alpha_t (T_t - 70)$$

and from pressure acting on the inside and outside of the tube as,

$$\Delta R_{to}^{pr} = \frac{P_i c}{E_t} \left[\frac{(2 - \nu) b^2}{c^2 - b^2} \right] - \frac{P_o c}{E_t} \left[\frac{(1 - 2\nu) c^2 + (1 + \nu) b^2}{c^2 - b^2} \right],$$

where: P_i = Internal primary side pressure, P_{pri} psi
 P_o = External secondary side pressure, P_{sec} psi
 b = Inside radius of tube = 0.33943 in.
 c = Outside radius of tube = 0.382 in.
 α_t = Coefficient of thermal expansion of tube, in/in/°F
 E_t = Modulus of Elasticity of tube, psi
 T_t = Temperature of tube, °F, and,
 ν = Poisson's Ratio of the material.

The thermal expansion of the hole ID is included in the finite element results and does not have to be expressly considered in the algebra; however, the expansion of the hole ID produced by pressure is given by:

$$\Delta R_{TS}^{pr} = \frac{P_i c}{E_{TS}} \left[\frac{d^2 + c^2}{d^2 - c^2} + \nu \right],$$

where: E_{TS} = Modulus of Elasticity of tubesheet, psi
 d = Outside radius of cylinder which provides the same radial stiffness as the tubesheet, that is, []^{a,c,e}.

If the unrestrained expansion of the tube OD is greater than the expansion of the tubesheet hole, then the tube and the tubesheet are in contact. The inward radial displacement of the outside surface of the tube produced by the contact pressure is given by: (Note: The use of the term δ in this section is unrelated its potential use elsewhere in this report.)

$$\delta_t = \frac{P_2 c}{E_t} \left[\frac{c^2 + b^2}{c^2 - b^2} - \nu \right]$$

The radial displacement of the inside surface of the tubesheet hole produced by the contact pressure between the tube and hole is given by:

$$\delta_{TS} = \frac{P_2 c}{E_{TS}} \left[\frac{d^2 + c^2}{d^2 - c^2} + \nu \right]$$

The equation for the contact pressure P_2 is obtained from:

$$\delta_{to} + \delta_{TS} = \Delta R_{to} - \Delta R_{TS} - \Delta R_{ROT}$$

where ΔR_{ROT} is the hole expansion produced by tubesheet rotations obtained from finite element results. The ΔR 's are:

$$\Delta R_{to} = c \alpha_t (T_t - 70) + \frac{P_{pri} c}{E_t} \left[\frac{(2 - \nu) b^2}{c^2 - b^2} \right] - \frac{P_{sec} c}{E_t} \left[\frac{(1 - 2\nu) c^2 + (1 + \nu) b^2}{c^2 - b^2} \right]$$

$$\Delta R_{TS} = \frac{P_{sec} c}{E_{TS}} \left[\frac{d^2 + c^2}{d^2 - c^2} + \nu \right]$$

The resulting equation is:

a,c,e

$$\left[\frac{P_{sec} c}{E_{TS}} \left[\frac{d^2 + c^2}{d^2 - c^2} + \nu \right] + \frac{P_{pri} c}{E_t} \left[\frac{(2 - \nu) b^2}{c^2 - b^2} \right] - \frac{P_{sec} c}{E_t} \left[\frac{(1 - 2\nu) c^2 + (1 + \nu) b^2}{c^2 - b^2} \right] - c \alpha_t (T_t - 70) - \Delta R_{ROT} \right]$$

For a given set of primary and secondary side pressures and temperatures, the above equation is solved for selected elevations in the tubesheet to obtain the contact pressures between the tube and tubesheet as a function of radius. The elevations selected ranged from the top to the bottom of the tubesheet. Negative "contact pressure" indicates a gap condition.

The OD of the tubesheet cylinder is equal to that of the cylindrical (simulate) collars (1.632 inches) designed to provide the same radial stiffness as the tubesheet, which was determined from a finite element analysis of a section of the tubesheet (References A.7 and A.8).

The tube inside and outside radii within the tubesheet are obtained by assuming a nominal diameter for the hole in the tubesheet (0.703 inch) and wall thinning in the tube equal to the average of that measured during hydraulic expansion tests. That thickness is 0.0396 inch for the tube. The following table lists the values used in the equations above, with the material properties evaluated at 600°F. (Note that the properties in the following sections are evaluated at the primary fluid temperature).

Thick Cylinder Equations Parameter	Value
b, inside tube radius, in.	0.3119
c, outside tube radius, in.	0.3515
d, outside radius of cylinder w/ same radial stiffness as TS, in.	[] ^{a,c,e}
α_t , coefficient of thermal expansion of tube, in/in °F	$7.83 \cdot 10^{-6}$
E_t , modulus of elasticity of tube, psi	$28.7 \cdot 10^6$
α_{TS} , coefficient of thermal expansion of tubesheet, in/in °F	$7.42 \cdot 10^{-6}$
E_{TS} , modulus of elasticity of tubesheet, psi	$26.4 \cdot 10^6$

A.1.4 Vogtle 1 & 2 Contact Pressures

A.1.4.1 Normal Operating Conditions

The loadings considered in the analysis are based on an umbrella set of conditions as defined in References A.9, A.10 and A.11. The current operating parameters from Reference A.9 are used. The temperatures and pressures for normal operating conditions at Vogtle 1 & 2 are bracketed by the following two cases:

Loading	Case 1 ⁽¹⁾	Case 2 ⁽²⁾
Primary Pressure	2235 psig	2235 psig
Secondary Pressure	810 psig	935 psig
Primary Fluid Temperature (T_{hot})	603.2°F	620.0°F
Secondary Fluid Temperature	521.8°F	538.4°F
⁽¹⁾ 0% Tube Plugging Case in Reference A.9.		
⁽²⁾ 10% Tube Plugging Case in Reference A.9		

The primary pressure [

]^{a,c,e}.

A.1.4.2 Faulted Conditions

Of the faulted conditions, Feedline Break (FLB) and Steamline Break (SLB) are the most limiting. FLB has a higher ΔP across the tubesheet, while the lower temperature of SLB results in less thermal tightening. Both cases are considered in this section.

Previous analyses have shown that FLB and SLB are the limiting faulted conditions, with tube lengths required to resist push out during a postulated loss of coolant accident (LOCA) typically less than one-fourth of the tube lengths required to resist pull out during FLB and SLB (References A.10 and A.11). Therefore LOCA was not considered in this analysis.

A.1.4.3 Feedline Break

The temperatures and pressures for the FLB event at Vogtle 1 & 2 are bracketed by the following two cases:

Loading	Case 1 ⁽¹⁾	Case 2 ⁽²⁾
Primary Pressure	2650 psig	2650 psig
Secondary Pressure	0 psig	0 psig
Primary Fluid Temperature (T _{hot})	579.2°F	596.0°F
Secondary Fluid Temperature	521.8°F	538.4°F
⁽¹⁾ 0% Tube Plugging Case in Reference A.9		
⁽²⁾ 10% Tube Plugging Case in Reference A.9		

The FLB condition [

] a.c.c.

A.1.4.4 Steam Line Break

As a result of SLB, the faulted SG will rapidly blow down to atmospheric pressure, resulting in a large ΔP across the tubes and tubesheet. The entire flow capacity of the auxiliary feedwater system would be delivered to the dry, hot shell side of the faulted SG. The primary side re-pressurizes to the pressurizer safety valve set pressure. The pertinent parameters are listed below. The combination of parameters yielding the most limiting results is used.

Primary Pressure	=	2560 psig
Secondary Pressure	=	0 psig
Primary Fluid Temperature (T _{hot})	=	420°F
Secondary Fluid Temperature	=	260°F

For this set of primary and secondary side pressures and temperatures, the equations derived in Section A.3 below are solved for the selected elevations in the tubesheet to obtain the contact pressures between the tube and tubesheet as a function of tubesheet radius for the hot leg.

A.1.4.5 Summary of FEA Results for Tube-to-Tubesheet Contact Pressures

For Vogtle 1 & 2, the contact pressures between the tube and tubesheet for various plant conditions are listed in Table A-5. Tube/Tubesheet Maximum & Minimum Contact Pressures and H* Depths for Vogtle 1 & 2 Steam Generators and plotted versus radius on Figure A-3

through Figure A-7. The application of these values to the determination of the required engagement length is discussed in Section A.3.

A.2 Tube-to-Tubesheet Hydraulic Expansion Joint Crevice Depth

The tube holes for Model F SGs were drilled from the bottom side of the tubesheet (standard practice), and the fabrication drawings required that the holes be deburred after drilling. Deburring effectively results in a chamfer of the hole and the maximum allowable depth for the chamfer was specified to be []^{a,c,c} inch. The tube installation hydraulic expansion process can also result in a short tapered crevice between the tube and the tubesheet at the secondary face of the tubesheet. This is an artifact of the expansion process equipment and its location within the tube at the time of application of the expansion pressure, and was a controlled dimension during fabrication. The maximum allowable crevice depth for the Vogtle 1 & 2 SGs was specified as []^{a,c,c} inch on the Reference A.12 drawing. In order to better quantify the requirements for controlling the crevice depth, and recognizing the stochastic nature of the manufacturing process, the hydraulic expansion procedure specification, Reference A.13, was stipulated statistical controls on the mean and the standard deviation of the crevice depth for a SG bundle. It was also stipulated that 99% of the population of crevice depths would be less than or equal to []^{a,c,c} inch although the allowable mean depth was increased. For the purpose of establishing the depth of engagement required to assure meeting both the structural and leak rate performance criteria for the Vogtle 1 & 2 SGs, the requirements of the latter procedure were considered and an allowance of 0.3 inch was selected for application. Although there can be circumstances where the crevice depth allowance would not be necessary, e.g., if the elevation of zero contact pressure from tubesheet bow induced tube hole dilation were below the 0.3 inch allowance depth, such instances would be expected to be rare and the allowance has been added to all structurally required depths for final application.

A.3 Determination of Required Engagement Length of the Tube in the Tubesheet

The elimination of a portion of the tube within the tubesheet from the in-service inspection (ISI) requirement constitutes a change in the location of the pressure boundary. The technical justification of the omission of the lower portion of the tube from examination relies on knowledge of the tube-to-tubesheet interference fit contact pressure at all elevations in the tube joint. In order to maintain consistency with other reports on this subject, the required length of engagement of the tube in the tubesheet to resist tube end-cap loads associated with the structural performance criteria is designated as H*. This length is based on structural requirements only and does not include any consideration of the potential leak rate, except perhaps in a supporting role with regard to the leak rate expectations relative to normal operating conditions. The contact pressure is used to calculate the magnitude of the force resisting pullout of the tube from the tubesheet over the H* length. It is also used in estimating the impact of changes in the contact pressure on potential primary-to-secondary leak rate during postulated accident conditions.

The end cap loads to be resisted during NOp and faulted conditions are:

Normal (maximum): $\pi \cdot (2235-810) \cdot (0.703)^2 / 4 = 553.11 \text{ lbs.}$

Faulted (FLB): $\pi \cdot 2650 \cdot (0.703)^2 / 4 = 1028.60 \text{ lbs.}$

Faulted (SLB): $\pi \cdot 2560 \cdot (0.703)^2 / 4 = 993.67 \text{ lbs.}$

To take advantage of the tube-to-tubesheet joint anchorage, it is necessary to demonstrate that [

] ^{a,c,c} The residual contact pressure from the tube installation was evaluated semi-empirically. It was determined by test for the as-fabricated condition and then analytically projected to the pertinent plant conditions. The tests involved pullout testing of tube-in-tubesheet specimens using thick collars to simulate the tubesheet for Model F tubes.

Seismic loads have also been considered, but they are not significant in the tube joint region of the tubes. The normal operation load is multiplied by a factor of 3 and the faulted condition loads by a factor of 1.4 to obtain the associated structural performance criteria.

The initial element in estimating the strength of the tube-to-tubesheet joint during normal operation or postulated accident conditions is the residual strength of the joint stemming from the expansion preload due to the manufacturing process, i.e., hydraulic expansion. During operation the preload increases because the thermal expansion of the tube is greater than that of the tubesheet and because a portion of the internal pressure in the tube is transmitted to the interface between the tube and the tubesheet. However, the tubesheet bows upward leading to a dilation of the tubesheet holes at the top of the tubesheet and a contraction at the bottom of the tubesheet when the primary-to-secondary pressure difference is positive. The dilation of the holes acts to reduce the contact pressure between the tubes and the tubesheet. The H* lengths are based on the pullout resistance associated with the net contact pressure during normal or accident conditions. The calculation of the residual strength involves a conservative approximation that the strength is uniformly distributed along the entire length of the tube. This leads to a lower bound estimate of the strength for the determination of H*.

For the partial-length RPC evaluation, tube-to-tubesheet contact pressure was calculated [

] ^{a,c,c}

The SG factory tube installation drawing specifies a [

] ^{a,c,c}

[]^{a,c,c}, to facilitate the tube weld to the cladding on the tubesheet face and it was omitted from the test. Following welding of the tube to the tubesheet, a full-length hydraulic expansion of the tube into the tubesheet is performed. The hydraulic expansion pressure range for the Model F SGs was approximately []^{a,c,c}. The majority of the test samples were expanded using a specified pressure of []^{a,c,c} to conservatively bound the lower expansion pressure limit used for SG fabrication.

Two testing programs were performed to determine the pullout resistance of Model F tube-to-tubesheet joints at []

[]^{a,c,c}. All of the test results are listed in Table A-13. The mechanical loading, or pullout, tests were run on a mechanical testing machine, []

[]^{a,c,c} The objective was to develop input information for analytically determining tube-to-tubesheet contact pressure and pullout resistance (lb/inch-axial). In this configuration, there is no contribution to tube-to-tubesheet contact pressure from tube internal pressurization. Internal pressurization also resists Poisson contraction associated with the axial load.

The data from the series of pullout tests are listed in Table A-13 and in Table A-14 for the 0.25 inch displacement data at 600°F. []

[]^{a,c,c}.

The force resisting pullout acting on a length of a tube between elevations h_1 and h_2 is given by:

$$F_i = (h_2 - h_1)F_{HE} + \mu \pi d \int_{h_1}^{h_2} P dh$$

where: F_{HE} = Resistance per length to pull out due to the installation hydraulic expansion,
 P = Contact pressure acting over the incremental length segment dh , and,
 μ = Coefficient of friction between the tube and tubesheet, conservatively assumed to be 0.2 for the pullout analysis to determine H^* .

The contact pressure is assumed to vary linearly between adjacent elevations in the top part of Table A-6 through Table A-10, so that between elevations L_1 and L_2 ,

$$P = P_1 + \frac{(P_2 - P_1)}{(L_2 - L_1)}(h - L_1)$$

or,

$$\left[\begin{array}{c} \text{a,c,e} \\ \text{ } \end{array} \right]$$

so that,

$$\left[\begin{array}{c} \text{a,c,e} \\ \text{ } \end{array} \right]$$

The latter equation was used to accumulate the force resisting pullout from the top of the tubesheet to each of the elevations listed in the lower parts of Table A-6 through Table A-10. The above equation is also used to find the minimum contact lengths needed to meet the pullout force requirements; a summary for the various zones is provided in Table A-11.

The top part of Table A-8 lists the contact pressures through the thickness at each of the radial sections for the SLB faulted condition. The last parameter row, " $h(0)$," of the central portion of the table lists the maximum tubesheet elevation at which the contact pressure is greater than or equal to zero. The above equation is used to accumulate the force resisting pull out from the top of the tubesheet to each of the elevations listed in the lower part of Table A-8. In Zone C for example, this length is 6.23 inches for the $1.4 \cdot \Delta P_{SLB}$ performance criterion which corresponds to a pullout force of 1391 lbs in the hot leg. The minimum contact length needed to meet the pullout force requirement of 1440 lbs for the Faulted (FLB) condition is less as is shown in Table A-9 and Table A-10. The H^* calculations for each loading condition at each of the radii considered are summarized in Table A-11. The H^* results for each zone are summarized in Table A-12. Therefore, the bounding condition for the determination of the H^* length is the SLB performance criterion.

In Zone D, The SLB performance criterion is controlling and the minimum contact length is 6.62 and 6.96 inches during a postulated SLB event for the hot and cold legs respectively, see Table A-12 which contains a summary for each of the zones. The smallest value occurs in Zone A where the tubesheet holes experience minimum dilation from the primary-to-secondary pressure difference.

A.4 References

- A.1 CN-SGDA-03-99, Evaluation of the Tube/Tubesheet Contact Pressures for Wolf Creek, Seabrook, and Vogtle 1 and 2 Model F Steam Generator,” September 2003.
- A.2 ASME Boiler and Pressure Vessel Code Section III, “Rules for Construction of Nuclear Power Plant Components,” 1989 Edition, The American Society of Mechanical Engineers, New York, NY.
- A.3 Porowski, J.S. and O’Donnell, W.J., “Elastic Design Methods for Perforated Plates,” Transactions of the ASME Journal of Engineering for Power, Vol. 100, p. 356, 1978.
- A.4 Slot, T., “Stress Analysis of Thick Perforated Plates,” PhD Thesis, Technomic Publishing Co., Westport, CN 1972.
- A.5 Computer Program WECAN/Plus, “User’s Manual,” 2nd Edition, Revision D, Westinghouse Government Services LLC, Cheswick, PA, May 1, 2000.
- A.6 Roark, R.J. and W.C. Young, “Formulas for Stress and Strain,” Fifth Edition, McGraw-Hill, New York, New York, USA, 1975.
- A.7 Nelson, L.A., “Reference for Model D Tubesheet Simulate [sic] of 1.800 Inch Diameter,” electronic mail, Westinghouse Electric Company LLC, Pittsburgh, PA, August 6, 2003.
- A.8 CN-SGDA-03-87 (Proprietary), “Evaluation of the Tube/Tubesheet Contact Pressures and H* for Model D5 Steam Generators at Byron, Braidwood, Catawba and Comanche Peak,” Westinghouse Electric Company LLC, Pittsburgh, PA, October 2003.
- A.9 CN-SGDA-03-85 (Proprietary), Rev. 1, “H*/P* Input for Model D5 and Model F Steam Generators,” September 2003.
- A.10 CN-SGDA-02-152 (Proprietary), Rev. 1, “Evaluation of the Tube-to-Tubesheet Contact Pressures for Callaway Model F Steam Generators,” Westinghouse Electric Company LLC, Pittsburgh, PA, March 2003.
- A.11 CN-SGDA-03-133 (Proprietary), Rev. 0, “Evaluation of the H* Zone Boundaries for Specific Model D-5 and Model F Steam Generators,” Westinghouse Electric Company LLC, Pittsburgh, PA, October 2003.
- A.12 Drawing 1511E64 (Proprietary), “Steam Generator Model F Tubing and Anti-Vibration Bar Assembly,” Westinghouse Electric Company LLC, Pittsburgh, PA, March 1979.
- A.13 Process Specification 81013 RM (Proprietary), Revision 9, “Hydraulic Tube Expansion,” Westinghouse Electric Company LLC, Pittsburgh, PA, August 1, 1980.
- A.14 Drawing 1104J40 (Proprietary), Rev. 4, “Steam Generator Model F Tube Bundle Assembly,” Westinghouse Electric Company LLC, Pittsburgh, PA, December 1978.

-
- A.15 NCE-88-271 (Proprietary), "Assessment of Tube-to-Tubesheet Joint Manufacturing Processes for Sizewell B Steam Generators Using Alloy 690 Tubing," Westinghouse Electric Company LLC, Pittsburgh, PA, November 1988.
- A.16 WCAP-14871 (Proprietary), "Vogtle Electric Generating Plant (VEGP) Steam Generator Tube-to-Tubesheet Joint Evaluation," Westinghouse Electric Company LLC, Pittsburgh, PA, May 1997.
- A.17 WNET-180 (Proprietary), Volume 11, "Model F Steam Generator Stress Report," Westinghouse Electric Company LLC, Pittsburgh, PA, September 1980.

Table A-1. Summary of Material Properties Alloy 600 Tube Material

Property	Temperature (°F)						
	70	200	300	400	500	600	700
Young's Modulus (psi·10 ⁶)	31.00	30.20	29.90	29.50	29.00	28.70	28.20
Thermal Expansion (in/in/°F·10 ⁻⁶)	6.90	7.20	7.40	7.57	7.70	7.82	7.94
Density (lb-sec ² /in ⁴ ·10 ⁻⁴)	7.94	7.92	7.90	7.89	7.87	7.85	7.83
Thermal Conductivity (Btu/sec-in-°F·10 ⁻⁴)	2.01	2.11	2.22	2.34	2.45	2.57	2.68
Specific Heat (Btu-in/lb-sec ² -°F)	41.2	42.6	43.9	44.9	45.6	47.0	47.9

Table A-2. Summary of Material Properties for SA-508 Class 2a Tubesheet Material

Property	Temperature (°F)						
	70	200	300	400	500	600	700
Young's Modulus (psi·10 ⁶)	29.20	28.50	28.00	27.40	27.00	26.40	25.30
Thermal Expansion (in/in/°F·10 ⁻⁶)	6.50	6.67	6.87	7.07	7.25	7.42	7.59
Density (lb-sec ² /in ⁴ ·10 ⁻⁴)	7.32	7.30	7.29	7.27	7.26	7.24	7.22
Thermal Conductivity (Btu/sec-in-°F·10 ⁻⁴)	5.49	5.56	5.53	5.46	5.35	5.19	5.02
Specific Heat (Btu-in/lb-sec ² -°F)	41.9	44.5	46.8	48.8	50.8	52.8	55.1

Table A-3. Summary of Material Properties SA-533 Grade A Class 2 Shell Material

Property	Temperature (°F)						
	70	200	300	400	500	600	700
Young's Modulus (psi·10 ⁶)	29.20	28.50	28.00	27.40	27.00	26.40	25.30
Thermal Expansion (in/in/°F·10 ⁻⁶)	7.06	7.25	7.43	7.58	7.70	7.83	7.94
Density (lb-sec ² /in ⁴ ·10 ⁻⁴)	7.32	7.30	7.283	7.265	7.248	7.23	7.211

Table A-4. Summary of Material Properties SA-216 Grade WCC Channelhead Material

Property	Temperature (°F)						
	70	200	300	400	500	600	700
Young's Modulus (psi·10 ⁶)	29.50	28.80	28.30	27.70	27.30	26.70	25.50
Thermal Expansion (in/in/°F·10 ⁻⁶)	5.53	5.89	6.26	6.61	6.91	7.17	7.41
Density (lb-sec ² /in ⁴ ·10 ⁻⁴)	7.32	7.30	7.29	7.27	7.26	7.24	7.22

Table A-5. Tube/Tubesheet Maximum & Minimum Contact Pressures
and H* Depths for Vogtle 1 & 2 Steam Generators

a,c,e

Notes:

- 1) Contact pressures values do not include the residual from the tube installation.
- 2) All H* values include a 0.3 inch allowance for the elevation of the BET relative to the TTS.

Table A-6. Cumulative Forces Resisting Pull Out from the TTS Vogtle 1 & 2
Hot Leg Normal Conditions – 0% SGTP, $P_{sec} = 810$ psig

a,c,e

Table A-7. Cumulative Forces Resisting Pull Out from the TTS Vogtle 1 & 2
Hot Leg Normal Conditions – 10% SGTP, $P_{sec} = 935$ psig

a,c,e

**Table A-8. Cumulative Forces Resisting Pull Out from the TTS Vogtle 1 & 2
Faulted (SLB) Conditions, Psec = 0 psig**

a,c,e

Table A-9. Cumulative Forces Resisting Pull Out from the TTS Vogtle 1 & 2
FLB Conditions, 0% SGTP

a,c,e

Table A-10. Cumulative Forces Resisting Pull Out from the TTS Vogtle 1 & 2
FLB Conditions, 10% SGTP

a,c,e

Table A-11. Summary of H* Calculations for Vogtle 1 & 2

**Table A-12. H* Summary Table
Structural Criteria Required Engagement**

Zone	Limiting Hot Leg Loading Condition	Engagement from TTS (inches)	
		Hot Leg	Cold Leg
A	$3 \cdot \Delta P_{NOp}^{(1,2)}$	2.15 ⁽³⁾	2.27 ⁽³⁾
B	$1.4 \cdot \Delta P_{SLB}^{(1,2)}$	4.26 ⁽³⁾	4.58 ^(3,4)
C	$1.4 \cdot \Delta P_{SLB}^{(1,2)}$	6.53 ⁽³⁾	6.85 ^(3,4)
D	$1.4 \cdot \Delta P_{SLB}^{(1,2)}$	6.62 ⁽³⁾	6.96 ^(3,4)
Notes: <ol style="list-style-type: none"> 1. Seismic loads have been considered and are not significant in the tube joint region (Reference A.17). 2. The scenario of tubes locked at support plates is not considered to be a credible event in Model F SGs as they are manufactured with stainless steel support plates. However, conservatively assuming that the tubes become locked at 100% power conditions, the maximum force induced in an active tube as the SG cools to room temperature is []^{a,c,e} 3. The specified H* values include an allowance of 0.3 inches to account for the BET location relative to the TTS. 4. $3 \cdot \Delta P_{NOp}$ conditions. 			

Table A-13. Model F Pullout Test Data

a,c,e

Table A-14. Model F 0.25 Inch Displacement Data at 600°F

a,c,e



Figure A-1. Definition of H* Zones (Vogtle Units 1 and 2).
(Zone D is the most inboard and Zone A the most outboard.)

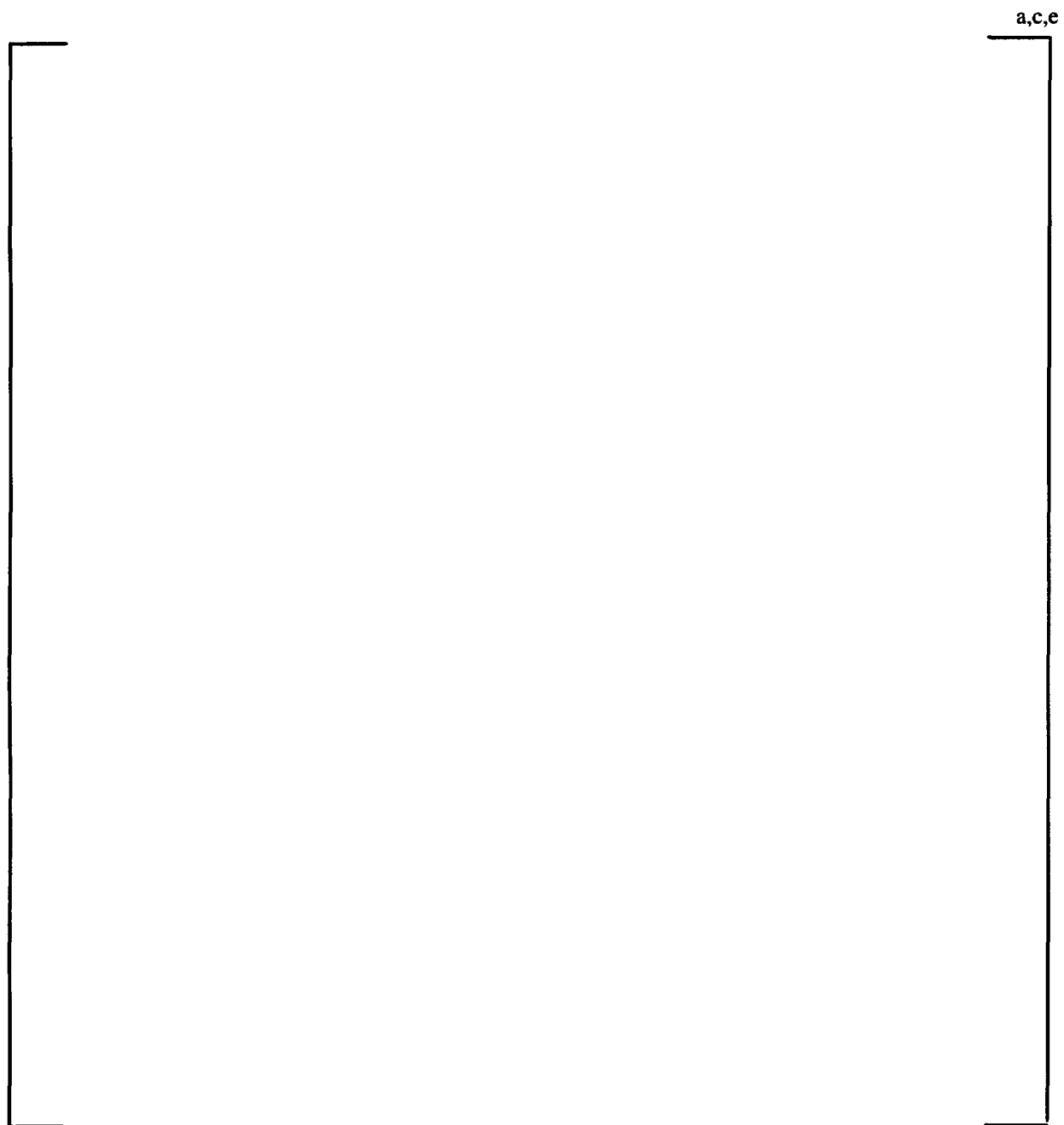


Figure A-2. Finite Element Model of Model F Tubesheet Region

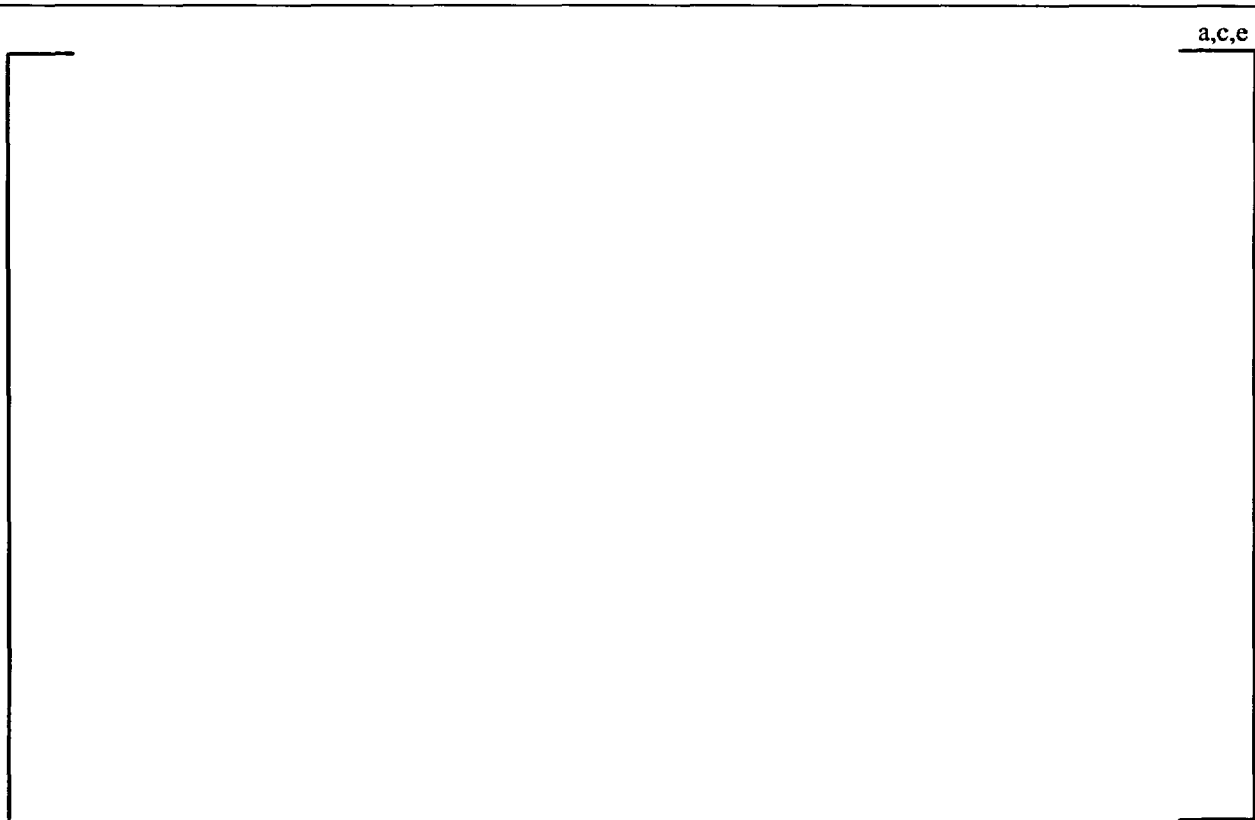


Figure A-3. Contact Pressures for NOp at Vogtle 1 & 2, 0% SGTP, $P_{sec} = 810$ psig



Figure A-4. Contact Pressures for NOp at Vogtle 1 & 2, 10% SGTP, $P_{sec} = 935$ psig

a,c,e



Figure A-5. Contact Pressures for SLB Faulted Condition at Vogtle 1 & 2

a,c,e



Figure A-6. Contact Pressures for FLB Condition at Vogtle 1 & 2, 0% SGTP

a,c,e

Figure A-7. Contact Pressures for FLB Condition at Vogtle 1 & 2, 10% SGTP